Volatility Components, Affine Restrictions, and Nonnormal Innovations

Peter CHRISTOFFERSEN
Desautels Faculty of Management, McGill University, Montreal, Quebec, H3A 1G5, Canada, Copenhagen Business School, and CREATES (*peter.christoffersen@mcgill.ca*)

Christian DORION
Department of Finance, HEC Montreal, Montreal, Quebec, H3T 2A7, Canada and McGill University (*christian.dorion@hec.ca*)

Kris JACOBS
C.T. Bauer College of Business, University of Houston, Houston, TX 77024, McGill University, and Tilburg University (*kjacobs@bauer.uh.edu*)

Yintian WANG
School of Economics and Management, Tsinghua University, Beijing 100083, China (*wangyt2@sem.tsinghua.edu.cn*)

Downloaded by [University of Toronto Libraries] at 07:32 18 November 2014

Here we assess the return fitting and option valuation performance of generalized autoregressive conditional heteroscedasticity (GARCH) models. We compare component versus GARCH(1, 1) models, affine versus nonaffine GARCH models, and conditionally normal versus nonnormal GED models. We find that nonaffine models dominate affine models in terms of both fitting returns and option valuation. For the affine models, we find strong evidence in favor of the component structure for both returns and options; for the nonaffine models, the evidence is less convincing in option valuation. The evidence in favor of the nonnormal GED models is strong when fitting daily returns, but not when valuing options.

KEY WORDS: Affine; Component model; Generalized autoregressive conditional heteroscedasticity; Long memory; Normality; Option valuation; Volatility.

1. INTRODUCTION

Following the groundbreaking work of Engle (1982) and Bollerslev (1986), generalized autoregressive conditional heteroscedasticity (GARCH) models have become an ubiquitous tool kit in empirical finance. In this article we assess the ability of eight different GARCH models to fit daily return dynamics and their ability to match market prices of options in a sample of close to 22,000 contracts. The eight models that we investigate differ along three dimensions.

First, we consider component models versus GARCH(1, 1) models. Engle and Lee (1999) were the first to develop a component GARCH model, which they built from the nonaffine NGARCH(1, 1) model analyzed by Engle and Ng (1993) and Duan (1995). Component GARCH models can be viewed as a convenient way of incorporating long-memory–like features into a short-memory model, at least for the horizons relevant for option valuation. Bollerslev and Mikkelsen (1999) find support for a long-memory GARCH option valuation model applied to long-maturity options. We consider options with up to 1-year maturity, for which the component models are likely to provide good approximations to long-memory processes. Maheu (2005) presented Monte Carlo evidence indicating that a component model similar to those presented in this article can capture long-memory volatility dynamics. Adrian and Rosenberg (2008) demonstrated the relevance of the component volatility structure for cross-sectional asset pricing.

Second, we consider nonaffine versus affine GARCH models. Most GARCH models are of a nonaffine form (see Christoffersen and Jacobs 2004), but Heston and Nandi (2000) developed a class of affine GARCH models. From the affine GARCH(1, 1) specification, Christoffersen et al. (2008) developed an affine GARCH component model, which we also consider herein. The affine GARCH(1, 1) model was compared with the nonaffine NGARCH(1, 1) model by Hsieh and Ritchken (2005), who found strong support for the nonaffine specification.

Third, we consider conditionally normal versus conditionally nonnormal models. In particular, we modify the foregoing four conditionally normal GARCH models by modeling the return shock using a generalized error distribution (GED). The GED distribution, suggested by Duan (1999) for its tractability in asset return modeling, conveniently nests the normal distribution. A skewed version of the GED distribution was developed by Theodossiou (2001) and has been used for option valuation by Lehnert (2003). Lehnert (2003) found support for a nonaffine EGARCH model with skewed GED shocks when comparing its option pricing performance with that of the affine GARCH(1, 1) model of Heston and Nandi (2000), which has normal innovations. We extend Lehnert's work by analyzing

© 2010 American Statistical Association
Journal of Business & Economic Statistics
October 2010, Vol. 28, No. 4
DOI: 10.1198/jbes.2009.06122

Downloaded by [University of Toronto Libraries] at 07:32 18 November 2014

whether the improvement comes from the nonaffine variance dynamic, from the nonnormal shocks, or from both features.

We estimate the resulting eight models using maximum likelihood (ML) estimation on S&P 500 returns. This empirical comparison allows us to compare the importance of three types of modeling assumptions: (a) the importance of the component structure versus the simpler and more parsimonious GARCH(1, 1) structure, (b) the restrictions of the affine structure, and (c) the importance of nonnormal return innovations. We find that the likelihood criterion based on return data strongly favors the component models in all cases, as well as the nonnormal return innovations. Although the affine models are not nested in the nonaffine models, comparing the likelihoods suggests that the nonaffine models fit the return data the best.

Using the ML estimates, we characterize key properties of each model: multiday variance forecasting functions, conditional volatility of variance paths, and conditional correlations between returns and variance. We find important differences between affine and nonaffine models suggesting that the nonaffine structure provides more flexibility in a parsimonious fashion. We also find substantial differences between GARCH(1, 1) and component models and between models with normal and nonnormal innovations.

When we use the estimated model parameters for option valuation, we again find strong support for the nonaffine variance specifications, but less evident support for the nonnormal return innovations. The component structure yields significant improvements in the affine class of models. In the nonaffine class, it yields improvements for long-maturity and out-of-the-money options.

The article is organized as follows. In Section 2 we develop the eight GARCH-based asset models that we investigate empirically in this work. In Section 3 we report the model estimates from daily returns and present some key dynamic properties of the models. In Section 4 we provide the theoretical mappings from physical to risk-neutral dynamics by applying the general approach of Duan (1999). In Section 5 we present the empirical results from using the GARCH models in option valuation, as well as an economic analysis of the option pricing errors. In Section 6 we conclude and suggest some promising avenues for future research.

2. ASSET RETURN MODELS

In this section we introduce the eight GARCH models to be used for option valuation. The eight models cover all of the possibilities in our three-way comparison: GARCH(1, 1) versus component GARCH, affine versus nonaffine GARCH, and normal versus GED-distributed return shocks.

2.1 The Affine GARCH (1, 1) Model With Normal Shocks

We first introduce the affine normal GARCH(1, 1) model of Heston and Nandi (2000). The return dynamics on the underlying asset are

$$\begin{aligned} R_{t+1} &\equiv \ln\left(\frac{S_{t+1}}{S_t}\right) = r + \lambda h_{t+1} + \sqrt{h_{t+1}} z_{t+1}, \\ h_{t+1} &= w + b' h_t + a(z_t - c\sqrt{h_t})^2, \end{aligned} \tag{1}$$

where S_{t+1} is the underlying asset price on the close of day $t+1$, r is the risk-free rate, λ is the price of risk, z_t is the iid N(0, 1) return shock, and h_{t+1} is the daily variance on day $t+1$ that is known at the end of day t. We refer to this model as the AGARCH(1, 1)-N model.

Note that c renders the variance response asymmetric to positive versus negative innovations in returns. If c is 0, then the variance dynamic is symmetric in z_t, and the conditional distribution of returns will be largely symmetric at all horizons, because the distribution of z_t is symmetric as well. In that case, the only source of asymmetry is the conditional mean return,

$$E_t[R_{t+1}] = r + \lambda h_{t+1}, \tag{2}$$

and this effect typically is very small in magnitude.

We next derive some features of the model that are particularly important for its performance in option valuation. The model's unconditional variance can be derived as

$$E[h_{t+1}] = \sigma^2 = \frac{w + a}{1 - ac^2 - b'}. \tag{3}$$

If we use this expression to substitute for w and also define variance persistence as $b = b' + ac^2$, then we can write

$$h_{t+1} = \sigma^2 + b(h_t - \sigma^2) + a(z_t^2 - 1 - 2c\sqrt{h_t} z_t). \tag{4}$$

The options that we analyze herein have maturities of between 1 week and 1 year. Thus it is important to gauge the model's properties at multiday horizons. In this regard, consider the conditional variance k days ahead,

$$E_t[h_{t+k}] = \sigma^2 + b^{k-1}(h_{t+1} - \sigma^2). \tag{5}$$

Although by design, the 1-day-ahead variance is deterministic in the GARCH models, the multiday variance is stochastic, and its distribution is important for option pricing as well. For 2 days ahead, the conditional variance of variance is easily derived from (4) as

$$\mathrm{Var}_t[h_{t+2}] = 2a^2 + 4a^2c^2 h_{t+1}. \tag{6}$$

Note that the variance of h_{t+2} is linear in h_{t+1}, which is a defining characteristic of the affine GARCH model. Note further that if c is 0, then the future variance will have constant conditional variance. This is at odds with the empirical evidence reported by, for example, Jones (2003), who found that the volatility of implied options volatility is higher when the level of implied options volatility is larger. Thus in the affine normal GARCH(1, 1) model, the c parameter is needed both to provide conditional variance of variance dynamics and to provide substantial conditional distribution asymmetry. This double duty may cause a tension in the model; we revisit this later.

The relationship between future variance and return is also of interest for option valuation. The so-called "leverage effect" was noted by Black (1976), who observed a negative correlation between volatility and returns. To describe this relationship, we consider the conditional covariance

$$\begin{aligned} &\mathrm{Cov}_t[R_{t+1}, h_{t+2}] \\ &\quad = E_t[\sqrt{h_{t+1}} z_{t+1} a(z_{t+1}^2 - 1 - 2c\sqrt{h_{t+1}} z_{t+1})] \\ &\quad = -2ach_{t+1}. \end{aligned} \tag{7}$$

Downloaded by [University of Toronto Libraries] at 07:32 18 November 2014

Note that because a must be strictly positive to ensure that the GARCH process is identified and positive, the sign of the leverage effect is driven entirely by c. From this conditional covariance, the conditional correlation is easily derived as

$$\text{Corr}_t[R_{t+1}, h_{t+2}] = \frac{-2c\sqrt{h_{t+1}}}{\sqrt{2+4c^2h_{t+1}}}. \tag{8}$$

Note that this conditional correlation is time-varying, which is a relatively unique property of the affine GARCH model.

2.2 The Affine GARCH Component Model With Normal Shocks

Many investigators (see, e.g., Bollerslev and Mikkelsen 1999) have found that simple exponential decay of the conditional variance to its unconditional value, in (5), is too fast. This motivates the affine normal GARCH component model developed by Christoffersen et al. (2008), who built on the work of Engle and Lee (1999) and Heston and Nandi (2000). The return and variance dynamics are now

$$\begin{aligned} R_{t+1} &= r + \lambda h_{t+1} + \sqrt{h_{t+1}}z_{t+1}, \\ h_{t+1} &= q_{t+1} + \beta(h_t - q_t) + \alpha(z_t^2 - 1 - 2\gamma_1\sqrt{h_t}z_t), \\ q_{t+1} &= \sigma^2 + \rho(q_t - \sigma^2) + \varphi(z_t^2 - 1 - 2\gamma_2\sqrt{h_t}z_t). \end{aligned} \tag{9}$$

Instead of mean-reverting to a constant unconditional variance, the conditional variance, h_{t+1}, now moves around a long-run component, q_{t+1}, which itself mean-reverts to the constant unconditional variance, σ^2. Furthermore, the two parameters γ_1 and γ_2 in the component model allow for a different degree of asymmetry in the two components, $(h_{t+1} - q_{t+1})$ and q_{t+1}. We refer to this model as the AGARCH(C)-N model.

The added dynamics in this model chiefly serve to generate more flexible dynamics in the multi-day-ahead conditional variance. We now have

$$\begin{aligned} E_t[h_{t+k}] &= E_t[q_{t+k} + (h_{t+k} - q_{t+k})] \\ &= \sigma^2 + \rho^{k-1}(q_{t+1} - \sigma^2) + \beta^{k-1}(h_{t+1} - q_{t+1}) \end{aligned} \tag{10}$$

which clearly allows for slower mean-reversion than (5). We refer to ρ as long-run persistence and to β as short-run persistence.

This component model also offers greater flexibility in the conditional variance of variance dynamic, which is now

$$\text{Var}_t[h_{t+2}] = 2(\alpha+\varphi)^2 + 4(\alpha\gamma_1 + \varphi\gamma_2)^2 h_{t+1} \tag{11}$$

so that the affine structure is preserved. The conditional covariance and correlation are

$$\text{Cov}_t[R_{t+1}, h_{t+2}] = -2(\alpha\gamma_1 + \varphi\gamma_2)h_{t+1} \tag{12}$$

and

$$\text{Corr}_t[R_{t+1}, h_{t+2}] = \frac{-2(\alpha\gamma_1 + \varphi\gamma_2)\sqrt{h_{t+1}}}{\sqrt{2(\alpha+\varphi)^2 + 4(\alpha\gamma_1 + \varphi\gamma_2)^2 h_{t+1}}}. \tag{13}$$

Note that in these formulas, $(\alpha + \varphi)$ has replaced a in the AGARCH(1, 1)-N model's formula, and similarly $(\gamma_1\alpha + \gamma_2\varphi)$ has replaced c. Thus, whereas c had to perform double duty (creating asymmetry and variance of variance dynamics) in the AGARCH(1, 1)-N model, the component model offers much added flexibility. The return asymmetry and variance of variance are now driven by two sources, parameterized by γ_1 and γ_2.

2.3 The Nonaffine GARCH(1, 1) Model With Normal Shocks

The benchmark NGARCH(1, 1)-N model of Engle and Ng (1993), which also was used for option valuation by Duan (1995), is defined as

$$\begin{aligned} R_{t+1} &= r + \lambda\sqrt{h_{t+1}} - \frac{1}{2}h_{t+1} + \sqrt{h_{t+1}}z_{t+1}, \\ h_{t+1} &= w + b'h_t + ah_t(z_t - c)^2. \end{aligned} \tag{14}$$

The parameter c again renders the variance response asymmetric to positive versus negative return shocks and creates asymmetry in the conditional distribution of multiday returns beyond that created by the conditional return mean,

$$E_t[R_{t+1}] = r + \lambda\sqrt{h_{t+1}} - \frac{1}{2}h_{t+1}. \tag{15}$$

Although this conditional mean specification differs from that used in the affine model, we use it because it will generate a risk-neutral conditional variance specification that is similar to the physical one, as we describe in Section 4. Similarly, the affine conditional mean specification in (2) will generate an affine conditional variance under the risk-neutral measure. We discuss this issue in more detail later in this article.

The unconditional variance is now

$$E[h_{t+1}] = \sigma^2 = \frac{w}{1 - b' - a(1+c^2)}. \tag{16}$$

Defining variance persistence as $b = b' + a(1 + c^2)$, we can rewrite the conditional variance as

$$h_{t+1} = \sigma^2 + b(h_t - \sigma^2) + ah_t(z_t^2 - 1 - 2cz_t). \tag{17}$$

The conditional variance k days ahead has the same form as in the affine model,

$$E_t[h_{t+k}] = \sigma^2 + b^{k-1}(h_{t+1} - \sigma^2), \tag{18}$$

and the conditional variance of variance can be derived from (17) as

$$\text{Var}_t[h_{t+2}] = a^2(2 + 4c^2)h_{t+1}^2. \tag{19}$$

Thus the variance of h_{t+2} is now quadratic in h_{t+1}, whereas it was linear in the affine model. Note also that even if c is 0 in the nonaffine model, the future variance will still have a dynamic variance, now driven by a.

The conditional covariance in this model is

$$\text{Cov}_t[R_{t+1}, h_{t+2}] = -2ach_{t+1}^{3/2}. \tag{20}$$

Thus the leverage effect again is driven by c, but now the covariance is nonlinear in h_{t+1}. Given the foregoing formula for conditional covariance, the conditional correlation is simply

$$\text{Corr}_t[R_{t+1}, h_{t+2}] = \frac{-2c}{\sqrt{2+4c^2}}. \tag{21}$$

Note that conditional correlation in the nonaffine model is constant, whereas it was time-varying in the affine model. Thus, along this dimension, the affine model seemingly offers more flexibility.

Downloaded by [University of Toronto Libraries] at 07:32 18 November 2014

2.4 The Nonaffine GARCH Component Model With Normal Shocks

As described in Section 2.2, this model is obtained by replacing the constant σ^2 in the NGARCH(1, 1)-N model with a time-varying, long-run component q_{t+1}. We write

$$\begin{aligned} R_{t+1} &= r + \lambda\sqrt{h_{t+1}} - \frac{1}{2}h_{t+1} + \sqrt{h_{t+1}}z_{t+1}, \\ h_{t+1} &= q_{t+1} + \beta(h_t - q_t) + \alpha h_t(z_t^2 - 1 - 2\gamma_1 z_t), \\ q_{t+1} &= \sigma^2 + \rho(q_t - \sigma^2) + \varphi h_t(z_t^2 - 1 - 2\gamma_2 z_t), \end{aligned} \tag{22}$$

and refer to this model as the NGARCH(C)-N model.

Once again, the added dynamics in this model chiefly serve to generate more flexible dynamics in the multi-day-ahead conditional variance. Here the multiday conditional variance is

$$\begin{aligned} E_t[h_{t+k}] &= E_t[q_{t+k} + (h_{t+k} - q_{t+k})] \\ &= \sigma^2 + \rho^{k-1}(q_{t+1} - \sigma^2) + \beta^{k-1}(h_{t+1} - q_{t+1}). \end{aligned} \tag{23}$$

The conditional variance of the variance dynamic is

$$\mathrm{Var}_t[h_{t+2}] = [2(\alpha + \varphi)^2 + 4(\alpha\gamma_1 + \varphi\gamma_2)^2]h_{t+1}^2, \tag{24}$$

which has contributions from both components and again is quadratic in h_{t+1}. The conditional covariance and correlation are

$$\mathrm{Cov}_t[R_{t+1}, h_{t+2}] = -2(\alpha\gamma_1 + \varphi\gamma_2)h_{t+1}^{3/2}, \tag{25}$$

which is nonlinear in h_t, and

$$\mathrm{Corr}_t[R_{t+1}, h_{t+2}] = \frac{-2(\alpha\gamma_1 + \varphi\gamma_2)}{\sqrt{2(\alpha + \varphi)^2 + 4(\alpha\gamma_1 + \varphi\gamma_2)^2}}, \tag{26}$$

which again is constant.

2.5 Generalized Error Distribution Shocks

The assumption that the daily return shock, z_t, is normally distributed is typically rejected empirically for daily asset returns. Our empirical analysis here is no exception. Note, however, that while the conditional 1-day distribution is normal when z_t is normal, the multiday distribution is not normal, and neither is the unconditional distribution. Thus the effect of the normal innovation assumption on option valuation in a GARCH model is not straightforward. Our analysis investigates whether these dynamics are sufficient to fit the underlying asset return as well as the option prices on the underlying asset, or whether the conditional normality assumption should be relaxed.

Following Duan (1999), we assume that the iid return shock, denoted by z_t in the normal case earlier, now follows the GED and is denoted by ζ_t. Once it is normalized to get a 0 mean and unit variance, we have the probability density function

$$g_v(\zeta) = \frac{v}{2^{1+1/v}\theta(v)\Gamma(1/v)}\exp\left(-\frac{1}{2}\left|\frac{\zeta}{\theta(v)}\right|^v\right) \quad \text{for } 0 < v \le \infty,$$

where Γ is the gamma function and $\theta(v) = (2^{-2/v}\Gamma(\frac{1}{v})/\Gamma(\frac{3}{v}))^{1/2}$.

The parameter v determines the thinness of the density tails. For $v < 2$, the density function has fatter tails than those of the normal distribution, and the opposite is true for $v > 2$. The expected simple return exists as long as $v > 1$, which thus is a natural lower bound in financial return applications.

The GED innovation ζ has a skewness of 0 and a kurtosis of $\kappa(v) = \Gamma(\frac{5}{v})\Gamma(\frac{1}{v})/\Gamma(\frac{3}{v})^2$. In the special case where $v = 2$, we get $\kappa(2) = 3$, and because $\Gamma(\frac{1}{2}) = \sqrt{\pi}$, we get

$$g_2(\zeta) = \frac{1}{\sqrt{2\pi}}\exp\left(-\frac{1}{2}\zeta^2\right)$$

so that the standardized GED conveniently nests the standard normal distribution that obtains when $v = 2$. Nelson (1991), Hamilton (1994), and Duan (1999) have provided more details on the properties of the GED distribution.

Replacing the normal distribution by the GED distribution in each of the four foregoing models provides four new models. The resulting eight models allow us to study the three dimensions of modeling in which we are interested: GARCH(1, 1) versus component GARCH, affine versus nonaffine GARCH, and normal versus nonnormal return shocks.

The GED distribution does not directly affect the variance persistence and, consequently, the multiday conditional variance in the first four models that we considered. The functional form for the conditional covariance is also unchanged in these models. But the excess kurtosis of the GED distribution does affect the conditional variance of variance in the four GED models; we now have

AGARCH(1, 1)-GED:

$$\mathrm{Var}_t(h_{t+2}) = (\kappa(v) - 1)a^2 + 4a^2c^2h_{t+1},$$

AGARCH(C)-GED:

$$\mathrm{Var}_t(h_{t+2}) = (\kappa(v) - 1)(\alpha + \varphi)^2 + 4(\alpha\gamma_1 + \varphi\gamma_2)^2h_{t+1},$$

NGARCH(1, 1)-GED:

$$\mathrm{Var}_t(h_{t+2}) = (\kappa(v) - 1 + 4c^2)a^2h_{t+1}^2,$$

NGARCH(C)-GED:

$$\mathrm{Var}_t(h_{t+2}) = \left[(\kappa(v) - 1)(\alpha + \varphi)^2 + 4(\alpha\gamma_1 + \varphi\gamma_2)^2\right]h_{t+1}^2,$$

where $\kappa(v) = \frac{\Gamma(5/v)\Gamma(1/v)}{\Gamma(3/v)^2}$ denotes the kurtosis under the GED distribution. This in turn affects the conditional correlation between return and volatility. In each of the conditional correlation formulas for the first four models, the 2 in the denominator is replaced by a $(\kappa(v) - 1)$ term.

3. ASSET RETURN EMPIRICS

In this section we present the empirical results from fitting our GARCH models to daily returns. First, we use ML estimation on a long time series of S&P 500 return data to estimate eight models: AGARCH(1, 1)-N, AGARCH(C)-N, NGARCH(1, 1)-N, NGARCH(C)-N, and the four GED-based models. We then discuss the parameter estimates and their implications for the salient properties of the models. The eight models allow us to make three types of comparisons: component models versus GARCH(1, 1) models, affine models versus nonaffine models, and nonnormal innovations versus normal innovations.

Downloaded by [University of Toronto Libraries] at 07:32 18 November 2014

3.1 Parameter Estimates From Daily Return Data

Table 1 presents the ML estimation results obtained using daily returns data from July 1, 1962 through December 31, 2001, obtained from CRSP. Standard errors, calculated as done by Bollerslev and Wooldridge (1992), are given in parentheses. The table reports the physical conditional variance parameters, as well as the price of risk, λ. The estimates of λ must be positive to guarantee positive excess log returns.

We use variance targeting to control the unconditional variance level across models, which is important for the subsequent option valuation exercise. We thus force the annualized return standard deviation to be 14.66%. This technique fixes the parameter w in each model, and thus we do not report standard errors for w in Table 1.

In the AGARCH(1, 1) cases, the unconditional variance is defined by $\sigma^2 = \frac{(w+a)}{(1-b)}$. Thus, if the data warrant a high a (perhaps to match variance of variance), then w will be small, to match σ^2. If left unconstrained, the w estimate may be negative, which yields the possibility of a negative conditional variance and thus causes problems in the subsequent Monte Carlo computation of option prices. Therefore, we constrain w to be positive in the estimation.

Table 1 reports the total variance persistence in each model. If we substitute out q_{t+1} and q_t from the h_{t+1} equation in the component models, then persistence can be computed as the sum of the coefficients on h_t and h_{t-1}. Thus the total persistence in the component models is $\rho + (1-\rho)\beta$. In the GARCH(1, 1) models, persistence is simply b. Note from Table 1 that while the GARCH(1, 1) models have high persistence, the persistence is even higher for each corresponding component model; this is particularly true for the affine models. The very large component variance persistence is driven by a large long-run component persistence, ρ, plus the contribution from [$(1-\rho)$ times] the less persistent short-run component, β.

In the GARCH(1, 1) models, the correlation between return and conditional variance is driven by c, which is, as expected, significantly positive in all cases. In the component models, the correlation is driven by a combination of γ_1 and γ_2, both of which are significantly positive in all four component models. Thus both the long-run and short-run components contribute to the overall correlation with the expected sign. The average conditional correlations between the return and conditional variance, reported in the third-to-last row of the table, are all negative, as expected. The results demonstrate that for each set of models, the component model displays a more pronounced leverage effect than its GARCH(1, 1) counterpart, in that the average correlation is more negative.

The variance of variance is driven mainly by the a parameter in the GARCH(1, 1) models and by the α and φ parameters in the component models. In the GED models, the ν parameter also contributes. Table 1 also reports the overall unconditional volatility of variance (annualized square root of variance of variance). Note again that in each case, the component

Table 1. Maximum likelihood estimation on daily S&P 500 returns, 1962–2001

	AGARCH-N		NGARCH-N		AGARCH-GED		NGARCH-GED	
	GARCH(1, 1)	Components	GARCH(1, 1)	Components	GARCH(1, 1)	Components	GARCH(1, 1)	Components
w	8.89E−21	7.02E−07	5.90E−07	1.74E−07	1.27E−09	5.89E−07	5.39E−07	1.64E−07
λ	0.00002	1.00495	0.03768	0.03390	0.56677	1.78607	0.03984	0.03674
	(1.83E−05)	(3.53E−06)	(8.62E−03)	(8.98E−03)	(1.42E−05)	(1.64E−04)	(8.30E−03)	(9.67E−03)
a, α	3.342E−06	2.132E−06	6.253E−02	3.696E−02	3.105E−06	1.705E−06	5.982E−02	3.071E−02
	(1.72E−07)	(1.40E−07)	(3.95E−03)	(3.45E−03)	(2.52E−04)	(1.35E−07)	(4.12E−03)	(4.72E−03)
b', β	0.89921	0.74928	0.90825	0.89262	0.90297	0.83454	0.91133	0.91320
	(2.47E−02)	(1.71E−04)	(5.30E−03)	(2.20E−02)	(6.90E−06)	(2.61E−05)	(5.71E−03)	(1.89E−02)
c, γ_1	135.7520	297.2247	0.5972	1.6588	139.7188	313.8362	0.6136	1.7759
	(2.47E−02)	(5.42E−05)	(4.67E−02)	(4.97E−02)	(1.70E−06)	(8.63E−04)	(5.77E−02)	(1.98E−01)
φ		1.739E−06		3.393E−02		1.524E−06		3.341E−02
		(4.84E−08)		(3.36E−03)		(1.10E−07)		(4.15E−03)
ρ		0.99176		0.99796		0.99309		0.99807
		(2.34E−06)		(5.21E−04)		(4.31E−04)		(6.13E−04)
γ_2		71.40695		0.38247		57.94967		0.38521
		(2.94E−05)		(4.76E−02)		(1.22E−03)		(5.64E−02)
ν					1.34637	1.41600	1.43298	1.45868
					(1.17E−07)	(3.04E−03)	(2.66E−02)	(2.84E−02)
Properties								
Log-likelihood	33,954	34,129	34,130	34,201	34,192	34,310	34,309	34,352
Annual volatility target	14.66	14.66	14.66	14.66	14.66	14.66	14.66	14.66
Total variance persistence	0.9608	0.9979	0.9931	0.9998	0.9636	0.9989	0.9937	0.9998
Empirical z kurtosis	8.9123	7.4070	6.6153	5.7752	9.1408	7.9727	6.6575	5.9424
Model z kurtosis	3.0000	3.0000	3.0000	3.0000	4.1797	3.9732	3.9274	3.8612
Annual vol. of variance	0.2289	0.3507	0.2497	0.3852	0.2341	0.3016	0.2725	0.3726
Average correlation	−0.8318	−0.8949	−0.6452	−0.8289	−0.7784	−0.8557	−0.5828	−0.7792

NOTE: We use daily total returns from July 1, 1962 to December 31, 2001 on the S&P 500 index to estimate the GARCH models using Maximum Likelihood. We use variance targeting to fix w so that the annual volatility in each model is 14.66%. Standard errors are calculated using Bollerslev and Wooldridge (1992). Annual vol. of variance refers to the sample mean of the annualized conditional volatility of variance path in each model. Correlation refers to the sample mean of the time-varying conditional correlation between variance and return in the affine models and to the constant model implied correlation in the nonaffine models.

Downloaded by [University of Toronto Libraries] at 07:32 18 November 2014

model has a larger volatility of variance than its GARCH(1, 1) counterpart. Thus three important empirical regularities emerge when comparing component models with their GARCH(1, 1) counterparts: the component models allow us to (simultaneously) capture a larger variance persistence, a larger leverage effect, and a larger volatility of variance than their GARCH(1, 1) counterparts.

Finally, Table 1 presents log-likelihood values for each model. In all cases, the component model has a significantly larger log-likelihood than the nested GARCH(1, 1) model. Comparing the GED models with their normal counterparts also shows that the GED-based models have significantly larger log-likelihood values. Thus this return-based analysis strongly favors the component models over the GARCH(1, 1) models and favors the GED models over the normal models. Although the affine and nonaffine models are not nested, a casual comparison of the log-likelihoods suggests that the nonaffine GARCH models also are strongly preferred over the affine GARCH models in all four cases.

3.2 Time Series Properties

To explore the asset return models further, here we plot various key dynamic properties of the models for the period 1989–2001. This period includes the dates for the option valuation exercise presented in Section 5.

Figure 1 plots the conditional volatility for the period 1989–2001. To be exact, the annualized conditional standard deviation is plotted as a percentage, that is, $100 * \sqrt{252 h_{t+1}}$. Note that the conditional volatility patterns across the four GARCH(1, 1) models in the left column and the corresponding four component models in the right column display some similarities. The models all capture the low volatility during the equity market runup in 1993–1998, preceded by higher volatility during the first Gulf War and the 1990–1991 recession. The LTCM and Russia crises in the fall of 1998 are evident, as is the higher volatility during the dot-com bust and the 2001 recession in the later part of the sample.

But Figure 1 also reveals some important differences among the models. The nonaffine models (in the second and fourth rows) appear to display much more variation in the conditional volatility during the second half of the sample than do the two affine models (in the first and third rows).

Figure 2 plots the annualized conditional volatility of variance path, $100 * 252\sqrt{\mathrm{Var}_t(h_{t+2})}$ for each of the four conditionally normal models in the top four panels. These plots confirm the findings presented in Figure 1. The nonaffine models in the second row of Figure 2 display a much larger volatility of variance than the affine models in the first row. This is true for both the GARCH(1, 1) models in the left column and the component models in the right column. The nonaffine models display a much larger volatility of variance during the first Gulf War and the 1990–1991 recession, and especially during the LTCM and Russia crises in the fall of 1998 and the dot-com bust in 2000–2002.

The bottom two rows of Figure 2 plot the conditional correlation path, $\mathrm{Corr}_t(R_{t+1}, h_{t+2})$, for each of our four conditionally normal models. Note that, as derived earlier, the nonaffine models imply a constant conditional correlation and thus exhibit a flat line in the plot. The affine models instead have time-varying correlation and imply a conditional correlation very close to -1 when economic events drive volatility up, as during, for example, the 1990–1991 recession and from 1999 onward. During the equity market runup in the mid 1990s, the conditional correlation implied by the affine models is much lower in magnitude.

The top row of Table 2 provides the correlation between conditional volatility in the AGARCH(1, 1)-N model and each of the other models. As Figure 1 suggests, these correlations are very high. Not surprisingly, the correlation with the AGARCH(1, 1)-GED model is virtually 1. The second row in Table 2 gives the correlation between the conditional volatility of variance in the AGARCH(1, 1)-N model and the other models. This correlation is still high when computed for other affine models but is now considerably lower for nonaffine models. The third row in Table 2 computes the correlation between the conditional return-variance correlation in the AGARCH(1, 1)-N model and the other models. Note again that this correlation is very high when computed for other affine models. It is, of course, zero for the nonaffine models, which have a constant conditional correlation over time.

3.3 Variance Term Structure Properties

While Figures 1 and 2 depict various aspects of the dynamics of the 1-day-ahead conditional distribution, Figure 3 captures the properties of the variance dynamics across longer horizons. In this figure, we plot the expected future conditional variance from 1 to 252 days ahead. The dashed lines in Figure 3 denote multiday variance forecasts starting from a low current spot variance corresponding to the 25th percentile of the path of variances from 1962 to 2001. The solid lines in Figure 3 denote multiday variance forecasts starting from a high current spot variance corresponding to the 75th percentile of the path of variances from 1962 to 2001. In the component models, the 25th and 75th percentiles are used for the current spot values for both components. The forecasts are normalized by the unconditional variance and shown in percentage terms, so that for each model, we are plotting $100 * (E_t[h_{t+k}] - \sigma^2)/\sigma^2$ against horizon k.

Figure 3 shows that the variance term structure properties vary strongly across models. In the AGARCH(1, 1) models, the relatively low daily variance persistence implies that the conditional variance forecasts converge to their unconditional levels after around 100 days. This is true for both the normal and GED version of the model. The AGARCH(C) models display some variation in variance forecasts across initial spot variance up until 252 days ahead, comparable to the variation displayed by the nonaffine GARCH(1, 1) models. The nonaffine component models display the most variation in variance forecasts at long horizons. These differences across models should have important implications for the option pricing properties.

4. OPTION VALUATION METHODOLOGY

To price options using the models developed earlier, we need to know the mapping between the physical return shocks, z_t,

Downloaded by [University of Toronto Libraries] at 07:32 18 November 2014

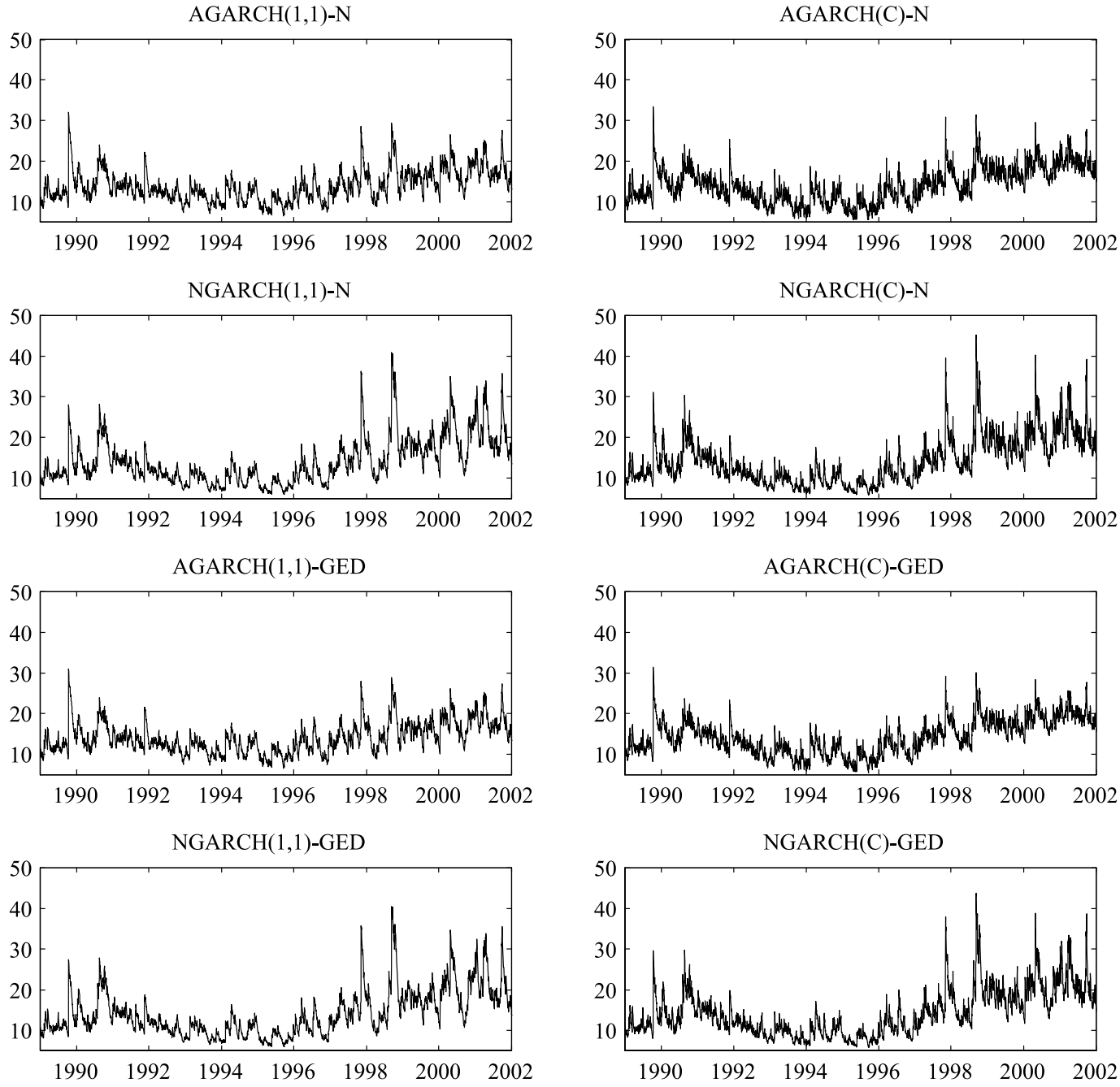

Figure 1. Conditional volatility paths. The annualized conditional volatility in percent, $100 * \sqrt{252 h_{t+1}}$, is plotted for each of the eight models that we consider. The parameter values for the underlying GARCH models are obtained from ML estimation on daily S&P 500 returns, as reported in Table 1.

and the risk-neutral return shocks. This mapping will allow us to use the physical asset return models developed earlier to simulate future stock prices from the risk-neutral distribution. These risk-adjusted prices can in turn be used to compute simulated option payoffs that once averaged and discounted using the risk-free rate, yield the current model option price.

Duan (1999) extended the normal case of Duan (1995) and derived a generalized local risk-neutral framework for option valuation in conditionally nonnormal GARCH models. As before, let z_{t+1} be iid normal under the physical measure and let z^*_{t+1} be iid normal under the risk-neutral measure. Define the mean-shift between the two measures by

$$\eta_{t+1} = z^*_{t+1} - z_{t+1}. \tag{27}$$

For a GED-distributed ζ_{t+1} shock, we can write the mapping as

$$\eta_{t+1} = z^*_{t+1} - \Phi^{-1}(G_v(\zeta_{t+1})),$$

where Φ^{-1} is the standard normal inverse cumulative distribution function (cdf) so that $z_{t+1} = \Phi^{-1}(G_v(\zeta_{t+1}))$ is normally distributed. We can then rewrite the linear normal mapping in (27) as a nonlinear GED mapping given by

$$\zeta_{t+1} = G_v^{-1}(\Phi(z^*_{t+1} - \eta_{t+1})). \tag{28}$$

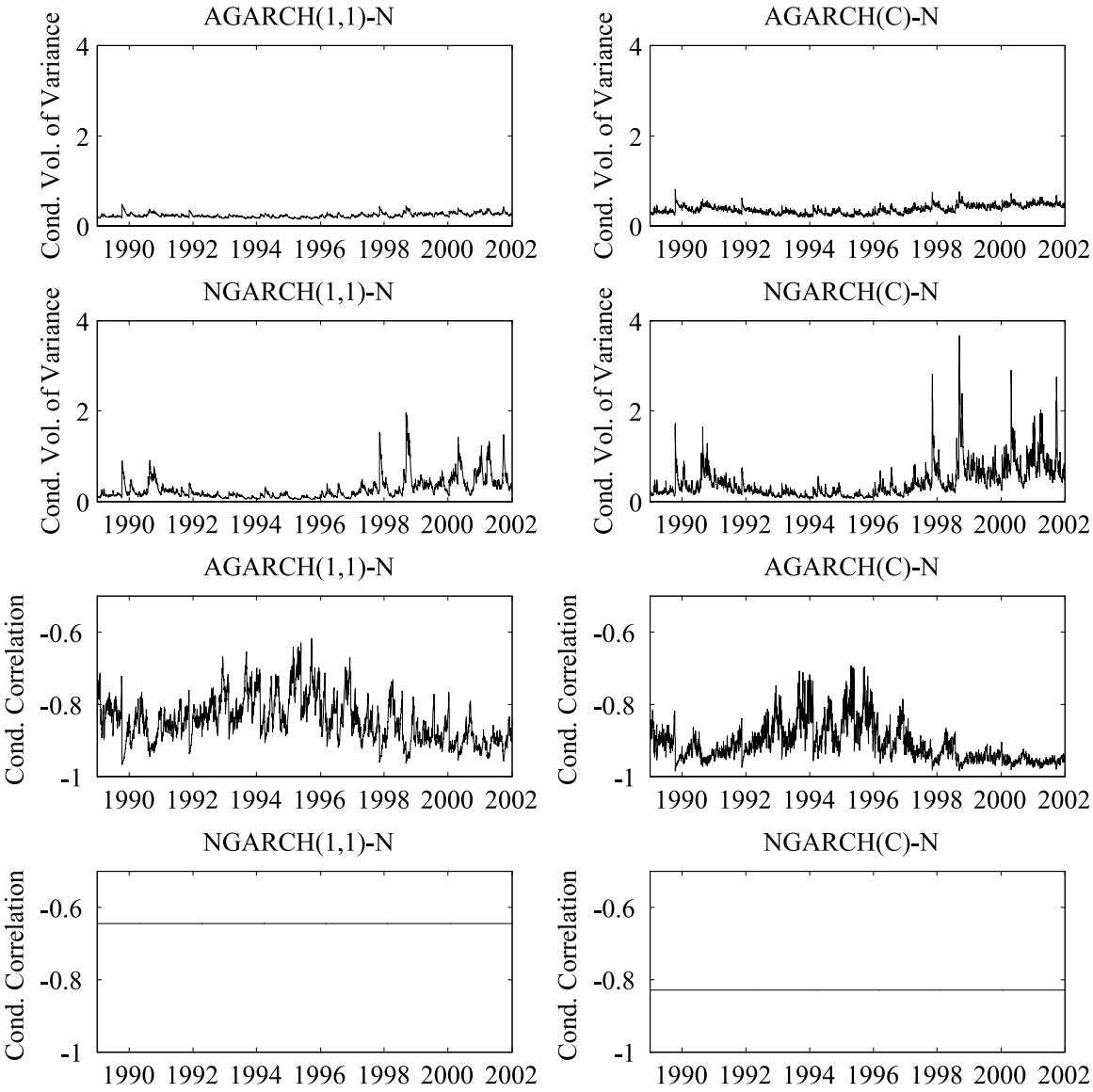

Figure 2. Conditional volatility of variance and conditional correlation paths. Conditionally normal models. We plot the annualized conditional volatility of variance path in percent, $100 * 252 * \sqrt{\text{Var}_t(h_{t+2})}$ (top four panels) and the conditional correlation path, $\text{Corr}_t(R_{t+1}, h_{t+2})$ (bottom four panels) for the four conditionally normal models. The parameter values for the underlying GARCH models are from Table 1.

Downloaded by [University of Toronto Libraries] at 07:32 18 November 2014

The derivation of the risk-neutral model requires solving for η_{t+1}. This is done by setting the conditionally expected risk-neutral asset return in each period equal to the risk-free rate. In general, we can write

$$\exp(r) = E_t^Q\left[\exp\left\{E_t[R_{t+1}] + \sqrt{h_{t+1}}G_v^{-1}(\Phi(z_{t+1}^* - \eta_{t+1}))\right\}\right],$$

where the normal case obtains for $v = 2$.

4.1 The Affine-Normal Models

Recall from before that in the affine models, the conditional return mean is defined as

$$E_t[R_{t+1}] = r + \lambda h_{t+1}. \tag{29}$$

In the normal case, of course, we have $G_2^{-1} = \Phi^{-1}$, so that the solution for η_{t+1} can be found as

$$\begin{aligned}
&\exp(r) = E_t^Q\left[\exp\{r + \lambda h_{t+1} + \sqrt{h_{t+1}}(z_{t+1}^* - \eta_{t+1})\}\right] \\
\Leftrightarrow\quad &1 = \exp(\lambda h_{t+1})\exp(-\eta_{t+1}\sqrt{h_{t+1}})\exp\left(\frac{1}{2}h_{t+1}\right) \\
\Leftrightarrow\quad &\eta_{t+1} = \left(\lambda + \frac{1}{2}\right)\sqrt{h_{t+1}}
\end{aligned}$$

so that

$$z_{t+1} = z_{t+1}^* - \left(\lambda + \frac{1}{2}\right)\sqrt{h_{t+1}}, \tag{30}$$

which corresponds to the mapping of Heston and Nandi (2000).

Future stock returns can now be simulated under the risk-neutral measure by substituting the shock transformation in (30) into the asset return models in (1) and (9). In the affine GARCH(1, 1) model, we get

$$\begin{aligned}
R_{t+1}^* &= r - \frac{1}{2}h_{t+1} + \sqrt{h_{t+1}}z_{t+1}^*, \\
h_{t+1} &= w + b'h_t + a(z_t^* - c^*\sqrt{h_t})^2,
\end{aligned} \tag{31}$$

Table 2. Model properties and *RMSE* from option valuation

	AGARCH-N		NGARCH-N		AGARCH-GED		NGARCH-GED	
	GARCH(1, 1)	Components	GARCH(1, 1)	Components	GARCH(1, 1)	Components	GARCH(1, 1)	Components
Correlation with AGARCH(1, 1)-N								
Conditional volatility	1.0000	0.9297	0.9373	0.9297	0.9995	0.9306	0.9365	0.9337
Conditional vol. of variance	1.0000	0.9267	0.7499	0.7571	0.9993	0.9283	0.7549	0.7667
Conditional correlation	1.0000	0.9113	0.0000	0.0000	0.9980	0.9270	0.0000	0.0000
Option *RMSE*								
Overall *RMSE* ($)	2.6927	1.8138	1.5875	1.3820	2.6819	1.7404	1.4599	1.4270
RMSE/Avr call price	0.0965	0.0650	0.0569	0.0495	0.0961	0.0623	0.0523	0.0511

NOTE: We compute the correlation between the AGARCH(1, 1) and each of the other models for the conditional volatility, the conditional volatility of variance, and the conditional correlation between return and variance. We then use the MLE parameters from Table 1 to risk neutralize the models and compute option prices. From the model option prices we compute the root mean squared error (*RMSE*) in dollars as well as divided by the average option price for the sample.

Downloaded by [University of Toronto Libraries] at 07:32 18 November 2014

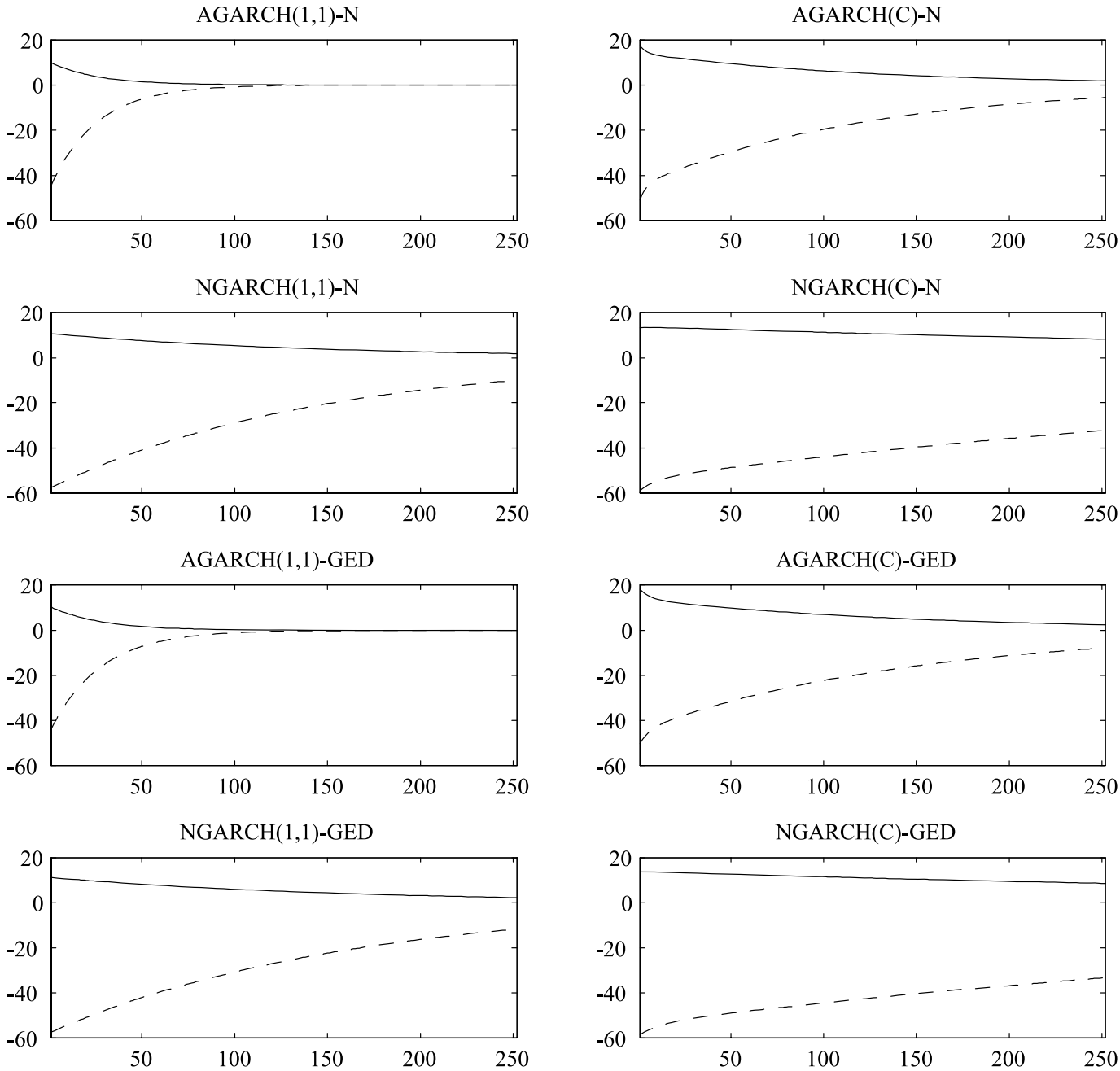

Figure 3. Variance forecasts across forecast horizons. We plot the normalized k-day-ahead variance forecast $100 * (E_t[h_{t+k}] - \sigma^2)/\sigma^2$ for a low initial spot variance (dashed line) and a high initial spot variance (solid line). See the text for details.

Downloaded by [University of Toronto Libraries] at 07:32 18 November 2014

where $z^*_{t+1} \sim \mathrm{N}(0,1)$ and $c^* = c + \lambda + \frac{1}{2}$. Note how the structure of the expected return, via its impact on the mapping from z_{t+1} to z^*_{t+1}, ultimately provides a risk-neutral volatility dynamic similar to the physical one.

4.2 The Nonaffine-Normal Models

In these models, we have

$$E_t[R_{t+1}] = r + \lambda\sqrt{h_{t+1}} - \frac{1}{2}h_{t+1} \tag{32}$$

so that the solution for η_{t+1} is found to be $\eta_{t+1} = \lambda$, which gives the mapping

$$z_{t+1} = z^*_{t+1} - \lambda, \tag{33}$$

which in turn corresponds to the mapping of Duan (1995).

Future stock returns can be simulated under the risk-neutral measure by substituting the shock transformation in (33) into the asset return models in (14) and (22). We get

$$\begin{aligned} R^*_{t+1} &= r - \frac{1}{2}h_{t+1} + \sqrt{h_{t+1}}z^*_{t+1}, \\ h_{t+1} &= w + b'h_t + ah_t(z^*_t - c^*)^2, \end{aligned} \tag{34}$$

where $z^*_{t+1} \sim \mathrm{N}(0,1)$ and $c^* = c + \lambda$. Note how once again, the structure of the expected return ultimately provides a nonaffine risk-neutral volatility dynamic similar to the nonaffine physical volatility dynamic.

4.3 The Affine GED Models

In the nonnormal case, an exact solution for η_{t+1} involves a prohibitively cumbersome numerical solution for η_{t+1} on every day and on every Monte Carlo path. Consequently, we develop the following approximation.

In the GED case, the parameter v determines the degree of nonnormality in the cdf G_v. When $v = 2$, we get normality, and when $v < 2$, we get fat tails. In the normal special case, we have $G_2^{-1}(\Phi(z)) = z$ for all z. Because the normal and GED are both symmetric, we know that $G_v^{-1}(\Phi(0)) = 0$ for all v. We use this to suggest the linear approximation

$$G_v^{-1}(\Phi(z)) \approx b_v z,$$

where b_v is easily found for a given value of v by fitting $\zeta_i = G_v^{-1}(\Phi(z_i))$ to z_i for a wide grid of z_i values. This approximation is motivated by the fact that the probability integral transform, $\zeta = G_v^{-1}(\Phi(z))$, is very close to linear for v values around the empirical estimates in Table 1.

With this approximation, we can write

$$\begin{aligned} 1 &= \exp(\lambda h_{t+1}) E^Q_t\left[\exp\left\{\sqrt{h_{t+1}}G^{-1}(\Phi(z^*_{t+1} - \eta_{t+1}))\right\}\right] \\ &\approx \exp(\lambda h_{t+1}) E^Q_t\left[\exp\{\sqrt{h_{t+1}}b_v(z^*_{t+1} - \eta_{t+1})\}\right] \\ &= \exp(\lambda h_{t+1}) \exp(-\eta_{t+1}\sqrt{h_{t+1}}b_v) \exp\left(\frac{1}{2}h_{t+1}b_v^2\right). \end{aligned}$$

Taking logs yields

$$0 = \lambda h_{t+1} - \eta_{t+1}\sqrt{h_{t+1}}b_v + \frac{1}{2}h_{t+1}b_v^2,$$

and solving for η_{t+1} yields

$$\eta_{t+1} = \left(\frac{\lambda}{b_v} + \frac{1}{2}b_v\right)\sqrt{h_{t+1}},$$

where, of course, the normal case obtains when $b_v = 1$.

The mapping between the physical GED and the risk-neutral normal shocks is now

$$\zeta_{t+1} = G_v^{-1}\left(\Phi\left(z^*_{t+1} - \left(\frac{\lambda}{b_v} + \frac{1}{2}b_v\right)\sqrt{h_{t+1}}\right)\right), \tag{35}$$

which can be substituted into the return dynamics for the AGARCH(1, 1)-GED and AGARCH(C)-GED models to get the risk-neutral processes.

Note that whereas the linear approximation greatly facilitates computing η_{t+1} in the GED models, computing option prices is still more cumbersome with GED innovations because of the frequent inversion of the GED cumulative distribution function in (35).

4.4 The Nonaffine GED Model

Using the nonaffine return drift but the same approximation of $G_v^{-1}(\Phi(\cdot))$ as before, we can write

$$\begin{aligned} 1 &= \exp\left(\lambda\sqrt{h_{t+1}} - \frac{1}{2}h_{t+1}\right) \\ &\quad \times E^Q_t\left[\exp\left\{\sqrt{h_{t+1}}G^{-1}(\Phi(z^*_{t+1} - \eta_{t+1}))\right\}\right] \\ &\approx \exp\left(\lambda\sqrt{h_{t+1}} - \frac{1}{2}h_{t+1}\right) E^Q_t\left[\exp\{\sqrt{h_{t+1}}b_v(z^*_{t+1} - \eta_{t+1})\}\right] \\ &= \exp\left(\lambda\sqrt{h_{t+1}} - \frac{1}{2}h_{t+1}\right) \exp(-\eta_{t+1}\sqrt{h_{t+1}}b_v) \\ &\quad \times \exp\left(\frac{1}{2}h_{t+1}b_v^2\right). \end{aligned}$$

Taking logs yields

$$0 = \lambda\sqrt{h_{t+1}} - \frac{1}{2}h_{t+1} - \eta_{t+1}\sqrt{h_{t+1}}b_v + \frac{1}{2}h_{t+1}b_v^2,$$

and solving for η_{t+1} yields

$$\eta_{t+1} = \frac{\lambda}{b_v} + \left(\frac{b_v}{2} - \frac{1}{2b_v}\right)\sqrt{h_{t+1}},$$

where, of course, the normal case again obtains when $b_v = 1$. The mapping between the shocks is then

$$\zeta_{t+1} = G_v^{-1}\left(\Phi\left(z^*_{t+1} - \frac{\lambda}{b_v} - \left(\frac{b_v}{2} - \frac{1}{2b_v}\right)\sqrt{h_{t+1}}\right)\right),$$

which can be substituted into the return dynamics for the NGARCH(1, 1)-GED and NGARCH(C)-GED models to get the risk-neutral processes.

Downloaded by [University of Toronto Libraries] at 07:32 18 November 2014

4.5 Monte Carlo Simulation

The European call option prices are computed via Monte Carlo, simulating the risk-neutral return process and computing the sample analog of the discounted risk neutral expectation. For a call option, $C_{t,T}$, quoted at the close of day t with maturity on day T and strike price X, we have

$$\begin{aligned} C_{t,T} &= \exp(-r(T-t))E_t^*[\max(S_T - X, 0)] \\ &\approx \exp(-r(T-t)) \\ &\quad \times \frac{1}{MC}\sum_{i=1}^{MC}\left[\max\left(S_t \exp\left(\sum_{\tau=1}^{T-t} R_{i,t+\tau}^*\right) - X, 0\right)\right], \end{aligned}$$

where $R_{i,t+\tau}^*$ denotes future daily log returns simulated under the risk-neutral measure. The subscript i refers to the ith out of a total of MC simulated paths.

To compute the option prices numerically, we use 20 affine matrix scrambles of 5,000 Sobol sequences each, for a total of 100,000 simulated paths. We use the empirical martingale method of Duan and Simonato (1998) to increase numerical efficiency.

To assess the accuracy of our Monte Carlo implementation, we use the model of Heston and Nandi (2000), for which quasi-analytical option prices are available via Fourier inversion of the conditional characteristic function. We compare these analytical option prices with the Monte Carlo prices for various strike prices, maturities, and volatility levels. We use the parameterization of the Heston–Nandi variance process from Table 1.

Figure 4 reports the results. The figure presents results for two maturities (1 month and 3 months) and for three spot volatility levels [6.48%, 12.11%, and 24.00%, equal to the minimum, median, and maximum model volatility of the AGARCH(1, 1)-N between January 1990 and December 1995]. In all cases, the Monte Carlo prices, denoted by "+," offer a very good approximation to the analytical prices, denoted by solid lines.

4.6 Option Valuation: Model Mechanics

Before turning to an empirical investigation of the various option valuation models, we analyze how the models differ in terms of option valuation by generating synthetic option prices for standardized moneyness, maturity, and volatility. This exercise provides us with intuition on how the various models are able to match option prices, and indicates in which dimensions different models fall short. We generate synthetic prices using the parameter estimates in Table 1, which reflect model properties at the optimum.

Figure 5 presents weekly synthetic prices for the four models with normal innovations. The results are very similar for the GED models, and thus we do not report these here. To include multiple maturities in the same figure, we convert the prices to Black–Scholes implied volatilities. The light-gray band plots results for a 1-month option, and the dark-gray band plots results for a 1-year option. The thickness of each band indicates the range of option prices generated by each model across the moneyness of the options. Each week, we value an option with moneyness (S/X) equal to 0.95 and 1.05; the thickness of the band indicates the difference between these two prices. Option prices are monotonic in moneyness, and all other determinants of price are kept constant; thus the width of the band is a function of moneyness only. Therefore, Figure 5 allows us to comment on differences between the models as a function of moneyness and maturity, as well as differences in model price over time, which are related to the volatility level.

We draw the following conclusions. First, the thickness of the bands clearly indicates that for longer-maturity options, the nonaffine models generate much more price variation across moneyness than the affine models. Second, differences between the models are more pronounced for longer-maturity options, which is not surprising; however, the nonaffine models value the 1-month options somewhat differently than the affine models. For comparison, we indicate the time path of the VIX by a black line. For the nonaffine models, the time path of the band for the 1-month option follows the VIX much more closely.

Third, some models—most notably the AGARCH(1, 1)-N—generate very little variation in long-maturity prices over the 1990–1995 sample. The nonaffine models and component models perform very differently in this respect. For example, it is striking that the time paths for the long-maturity and short-maturity bands are much more correlated for the NGARCH(C)-N model than for the other models. Thus we conclude that models strongly differ in their pricing results under changing (volatility) conditions. The nonaffine models allow for more variation in prices as a function of volatility, such as, for example, higher prices in the more volatile 1990–1991 period. But obtaining prices for long-maturity options that are more correlated with those of shorter-maturity options requires component models.

Figure 6 provides further insight by presenting plots of synthetic 1-month option prices as a function of moneyness and volatility. To accentuate differences between models, we plot the differences between model prices and Black–Scholes prices. Because of space constraints, we provide results only for the nonaffine models with normal innovations.

While the volatility level on the horizontal axis in the figure fixes the spot variance h_t in the models, we still need to fix the long-run variance factor, q_t, in the component models. We proceed as follows. In the top right panel of Figure 6, we set q_t, so that the ratio q_t/h_t corresponds to the 90th percentile of the historical ratio, thus generating a relatively high long-run variance factor. In the bottom right panel of Figure 6, we set q_t, so that the ratio q_t/h_t corresponds to the 10th percentile of the historical ratio, generating a low long-run variance factor. Note again that the overall variance, h_t, is kept the same across models. Thus the values for the two GARCH(1, 1) models in the left panels are identical. Finally, note that while option model prices increase as a function of volatility, of course the same need not apply to the model price net of the Black–Scholes price.

Figure 6 shows large differences between the GARCH(1, 1) and the component models when the long-run variance factor is high. The nonaffine GARCH(1, 1) model generates larger differences with Black–Scholes when volatility is high; however, this difference is dwarfed by the difference between the GARCH(1, 1) and component models when the long-run variance component is high.

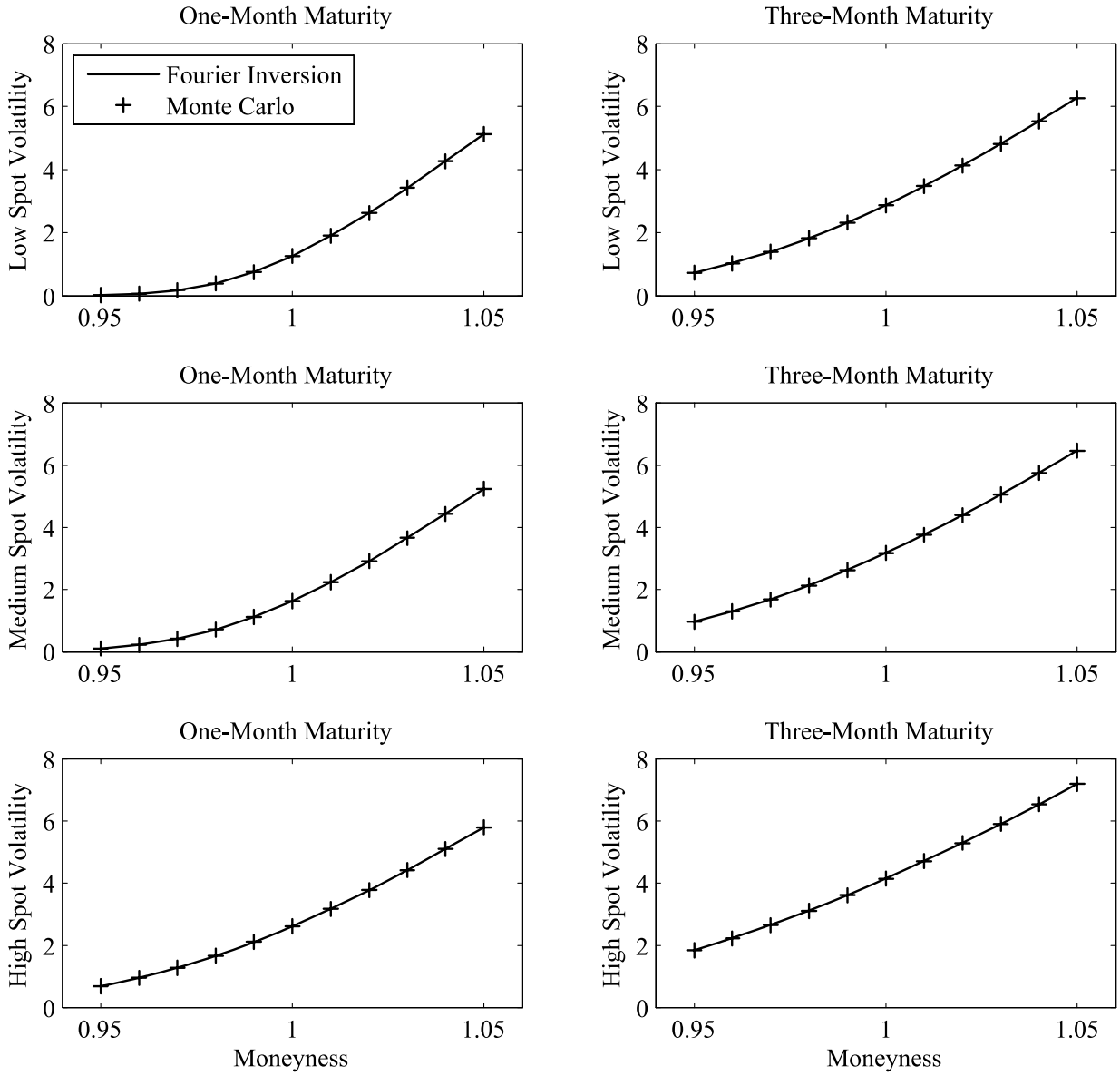

Figure 4. Accuracy of Monte Carlo simulated prices. Using the AGARCH(1, 1)-N model and the parameters from Table 1, we compare quasi-analytical option prices from Fourier inversion (solid) to the Monte Carlo prices ("+") for various strike prices, maturities, and volatility levels. The three spot volatility levels are 6.48%, 12.11%, and 24.00%, corresponding to the minimum, median, and maximum model volatility of the model between 1990 and 1995.

Downloaded by [University of Toronto Libraries] at 07:32 18 November 2014

The bottom-right panel of Figure 6 shows the case where the long-run variance factor is low. Note that we have kept the overall volatility the same as in the top-right panel. When the long-run variance factor is relatively low, the component models generate prices that are even closer to Black–Scholes than those generated by the GARCH(1, 1) models.

The overall conclusion from Figure 6 is that the component structure gives additional flexibility in generating option prices that vary not only as a function of the overall level of volatility, but also as a function of the composition of overall volatility into short-run and long-run components.

5. OPTION VALUATION EMPIRICS

We are now ready to use the eight models estimated in Section 2 and the transformation to risk-neutrality in Section 4 to assess the performance of the models for option valuation. In this section we first introduce the options data, then use each of our eight models to price the option contracts and compare model and market prices for various maturities, strike prices, and sample years. We then report an economic analysis of the errors, and finally investigate alternative estimation strategies.

5.1 Option Data

We use 6 years of S&P 500 call option data covering the period 1990–1995. Starting from the raw data from the Berkeley option data base, we apply standard filters following Bakshi, Cao, and Chen (1997). We use only options with more than 7 days to maturity. We also use only Wednesday options data. Wednesday is the day of the week least likely to be a

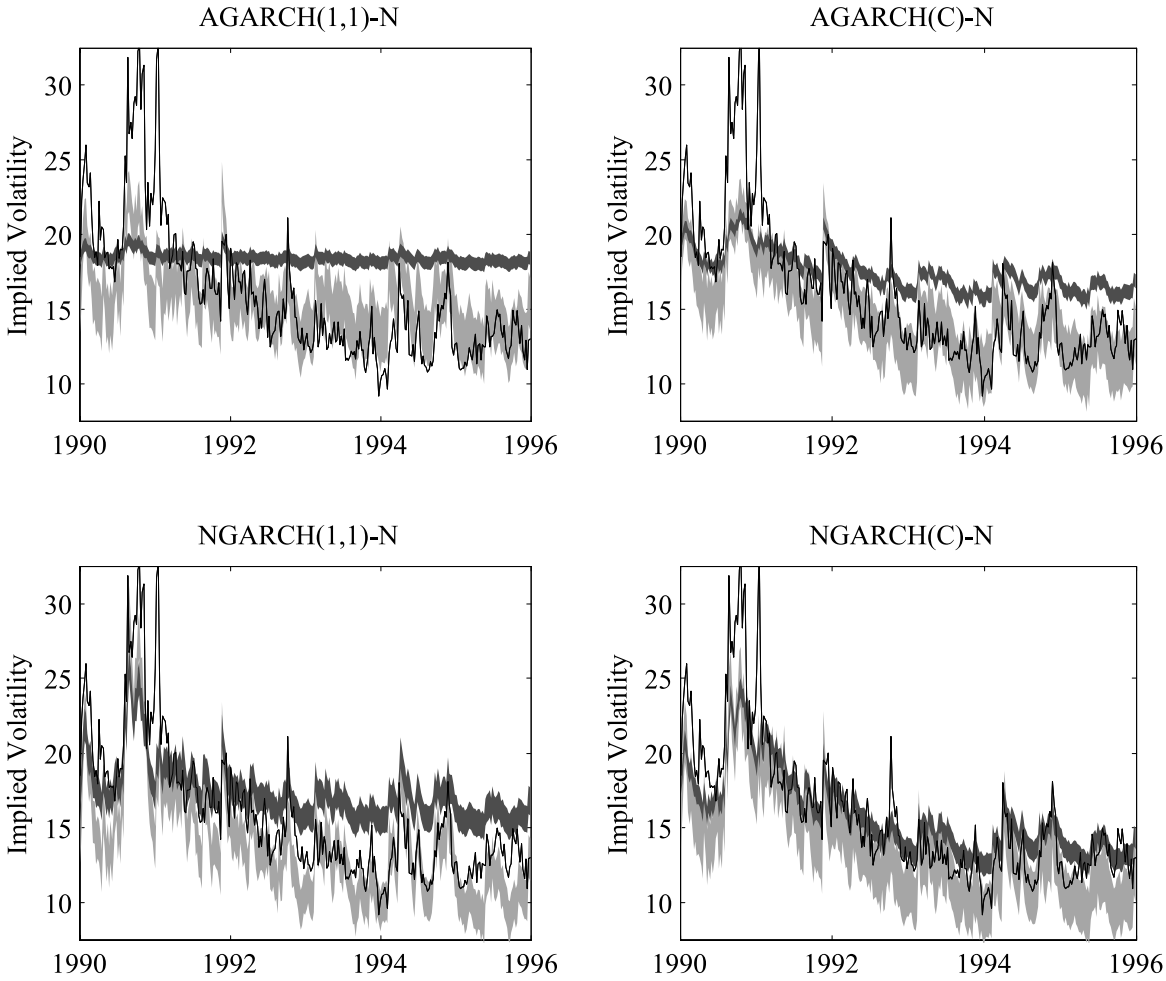

Figure 5. Synthetic option-implied volatilities across time. We plot weekly synthetic implied Black–Scholes volatilities for the four models with normal innovations. The light-gray band plots the results for a 1-month option, and the dark-gray band plots the results for a 1-year option. The black line denotes the VIX index. Each week, we value an option with moneyness (S/X) equal to 0.95 and 1.05; the thickness of the band indicates the difference between these two prices.

Downloaded by [University of Toronto Libraries] at 07:32 18 November 2014

holiday, and is also less likely than other days, such as Monday and Friday, to be affected by day-of-the-week effects. If Wednesday is a holiday, then we use the next trading day. Using only Wednesday data allows us to study a fairly long time series, which is useful considering the highly persistent volatility processes.

Our sample comprises 21,752 options with a wide range of moneyness and maturity. The average overall price is \$27.91. The data have been described in more detail by Christoffersen et al. (2008).

The implied Black–Scholes volatilities display strong evidence of a "smirk" or "skew" across strikes, with higher implied volatility for in-the-money calls than at-the-money calls, and this holds for all maturities. This empirical regularity illustrates that the Black–Scholes option valuation formula, which assumes a constant per period volatility across time, maturity, and strike prices, will result in systematic pricing errors, which motivates the use of GARCH models for option valuation.

5.2 Overall Option Valuation Results

When calculating option prices according to the eight GARCH models, we use the ML estimation parameters in Table 1 transformed to the risk-neutral measure. We use these risk-neutral parameters, along with the conditional variance paths from Figure 1 as inputs into the option pricing formula. In the case of the nonaffine and/or nonnormal models, Monte Carlo simulation is required to calculate the price. In the case of the normal affine models, numerical integration solutions exist; however, to ensure that the results are not driven by the numerical pricing technique, we use Monte Carlo simulation using the same set of random numbers for all models.

The overall *RMSE*s for the eight GARCH models are reported in the next to last row of Table 2. The root mean squared error (*RMSE*) is computed as

$$RMSE = \sqrt{\frac{1}{N}\sum_{i,t}(C_{i,t}^{Market} - C_{i,t}^{Model})^2},$$

where the summation is over contract i observed on day t and where N is equal to 21,752, the total number of option contracts in the sample. The last row in Table 2 normalizes the *RMSE* by dividing it by the average call price in the sample.

Note first that the best overall model (i.e., that with the lowest *RMSE*) is the NGARCH(C)-N, with an *RMSE* of 1.38, followed closely by the NGARCH(C)-GED, with an *RMSE* of

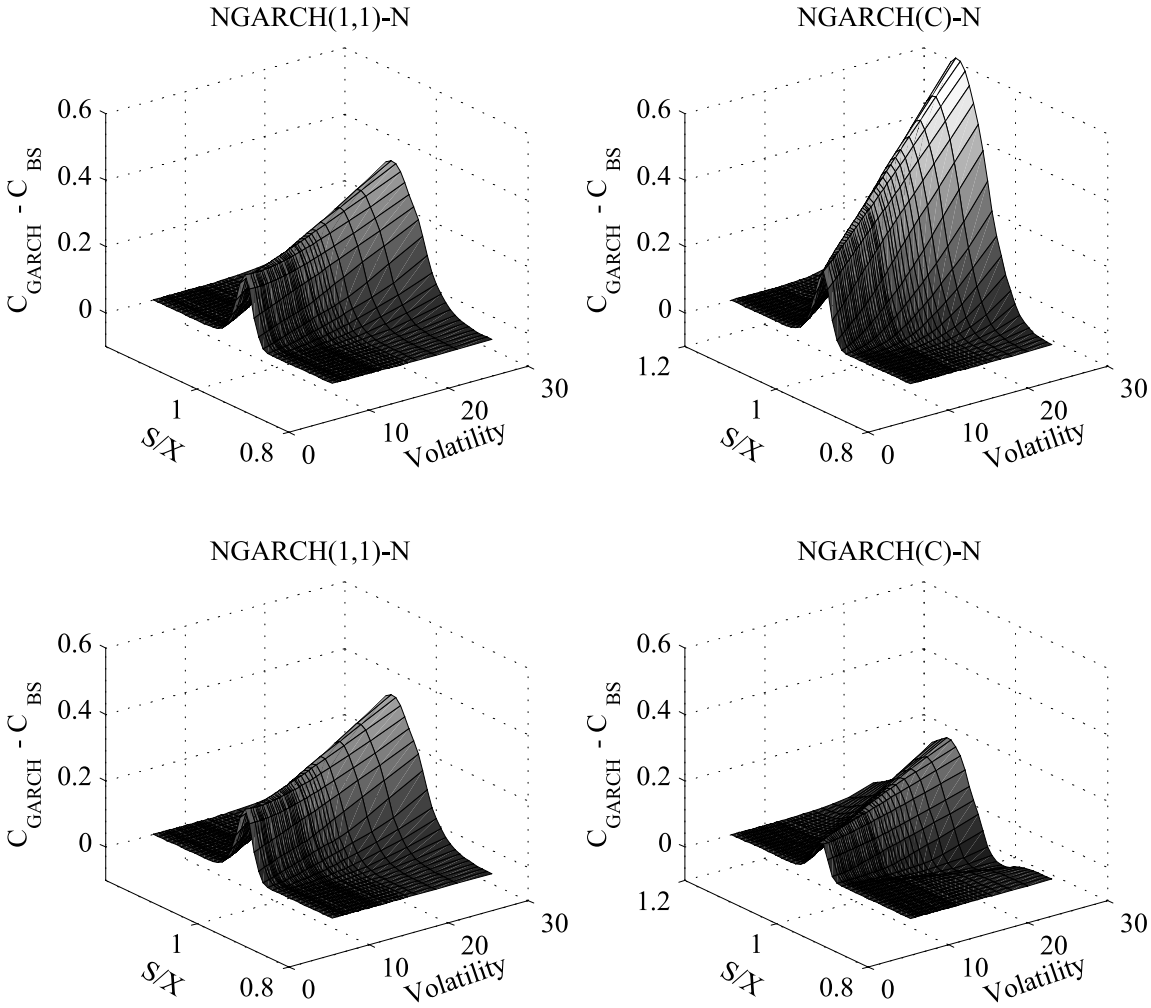

Figure 6. Synthetic NGARCH-N option prices across moneyness (S/X) and volatility levels. For the NGARCH normal models, we plot the synthetic model option price less the Black–Scholes price as a function of moneyness (S/X) and volatility for options with 1 month to maturity. For the component model, we set the proportion of the long-run variance factor, q_t, to the total variance, h_t, equal to the 90th percentile (top right) and the 10th percentile (bottom right) of its historical distribution.

Downloaded by [University of Toronto Libraries] at 07:32 18 November 2014

1.43. The two nonaffine GARCH(1, 1) models also perform relatively well, with *RMSE*s of 1.46 in the GED case and 1.59 in the normal case. The affine models as a group perform worse than the nonaffine models. The *RMSE* of the AGARCH(C)-GED model is 1.74, and that of the AGARCH(C)-N model is 1.81. The two affine GARCH(1, 1) models perform the worst, with an *RMSE* of 2.68 in the GED case and 2.69 in the normal case.

These overall *RMSE* results allow us to make comparisons in three dimensions: affine versus nonaffine variance dynamics, GED versus normal shocks, and GARCH(1, 1) versus component variance models.

First, as noted earlier, we see that nonaffine models perform much better than affine models. This is true both for GARCH(1, 1) and component models and for GED and normal shocks. Thus our results confirm and extend those of Hsieh and Ritchken (2005) who compared an affine model and a nonaffine model in the GARCH(1, 1) case with normal shocks.

Second, we see that GED models perform only marginally better than normal models. The greatest improvement is in the NGARCH(1, 1) case, where the *RMSE* drops from 1.59 to 1.46 when going from GED to normal shocks. In the other pairwise comparisons, the difference between the GED and the normal *RMSE* is around 5 cents.

Third, we see that the component structure offers large improvements in fit for the affine class of models but more modest improvements in the nonaffine class of models. For the affine models, the *RMSE* drops from 2.69 to 1.81 for normal shocks and from 2.68 to 1.74 for GED shocks, whereas for the nonaffine models, the RMSE drops from 1.59 to 1.38 for normal shocks and from 1.46 to 1.43 for GED shocks.

Recall now the main findings in terms of daily return log-likelihood values in Table 1. In all cases, the component model has a significantly larger log-likelihood than the nested GARCH(1, 1). Comparing the GED models with their normal counterparts reveals that the GED-based models have significantly larger log-likelihood values. The log-likelihood values also suggest that the nonaffine GARCH models are strongly preferred over the affine GARCH models. The option-based results support the return-based improvement of nonaffine models over affine models. They also support the component model

improvements over GARCH(1, 1) for affine models, but somewhat less so for nonaffine models. While the GED offers drastic improvements in the return-based likelihood analysis, the improvements offered in option valuation are much more modest. The normal GARCH models may offer sufficient nonnormality in the multiday distribution, or, alternatively, the GED specification may not be adequate for the purpose of option valuation.

5.3 Results by Moneyness, Maturity, and Volatility Level

Figure 7 provides more intuition for the models' performance by plotting the *RMSE* and bias results as a function of moneyness (i.e., index value over strike value), maturity, and volatility level. Note that the scales differ across panels in Figure 7, to focus on the differences between models.

The plots in the top row of Figure 7 show *RMSE* and bias for each model using six moneyness bins. *RMSE* is presented in the left panel, and bias is shown in the right panel. Bias is defined as average market price minus model price. In each panel, the solid line represents the model with normal innovations and the dashed line represents the model with GED innovations. The bias plots indicate that model prices are generally larger than market prices, especially for out-of-the money call options. An important observation is that while the GED models outperform the models with normal innovations, the differences in performance are small, and for many models are almost nonexistent in most of the bins. This confirms the results presented in Section 5.2. But the GED models slightly outperform the models with normal innovations for out-of-the-money options, where nonnormality has more impact. Furthermore, while affine models perform similar to nonaffine models for in-the-money options, nonaffine models perform much better for

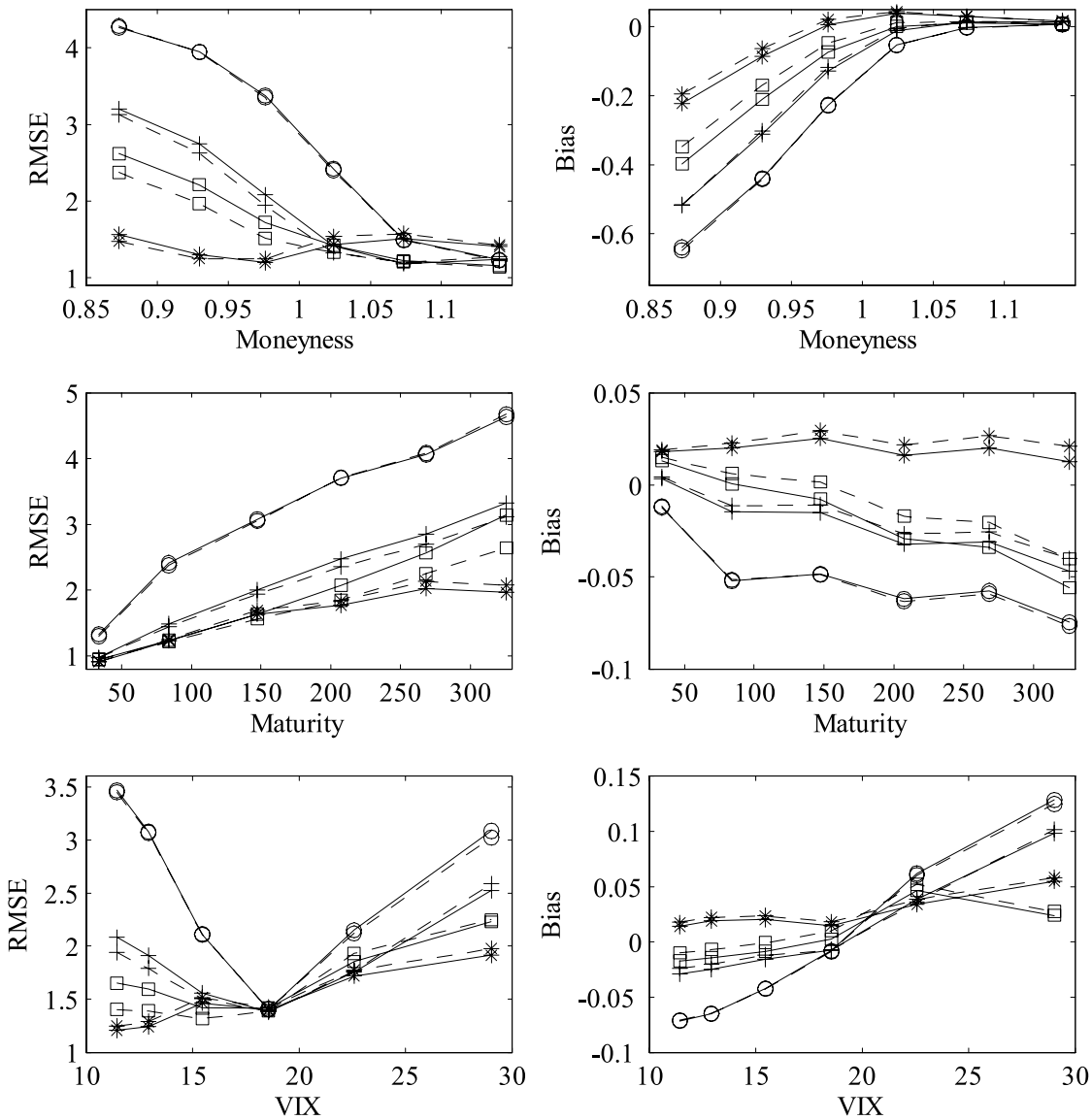

Figure 7. Option *RMSE* and bias against moneyness, maturity, and VIX level. We plot *RMSE* (left column) and *bias* (right column) for each model using six moneyness bins (top row), maturity bins (middle row), and VIX levels (bottom row). Normal models are indicated by solid lines; GED models, by dashed lines. AGARCH(1, 1) is marked with "∘," NGARCH(1, 1) with "□," AGARCH(C) with "+," and NGARCH(C) with "*."

Downloaded by [University of Toronto Libraries] at 07:32 18 November 2014

Downloaded by [University of Toronto Libraries] at 07:32 18 November 2014

out-of-the money and at-the-money options. The affine models perform particularly poorly for out-of-the money options, perhaps not providing sufficient nonnormality at the relevant horizons. Differences across models also are generally larger for out-of-the-money options, driving the overall *RMSE* result. Finally, the nonaffine component models significantly outperform the NGARCH(1, 1) models, suggesting that in the moneyness dimension, both the nonaffine structure and the component structure are needed.

The plots in the middle row of Figure 7 strongly suggest that both components and a nonaffine structure are also needed in the maturity dimension. The plots show *RMSE* and bias for each model using six maturity bins. The nonaffine component models significantly outperform the affine component models and the nonaffine GARCH(1, 1) models, suggesting that the nonaffine structure and the component structure by themselves are not sufficient to capture the richness of the data. The other important conclusion is, of course, that differences in model performance appear mainly at long maturities. The affine component models do well for the shortest maturities, but the nonaffine component and GARCH(1, 1) models perform better than the affine models at longer maturities. The relative lack of flexibility in the longer-term variance dynamics shown in Figure 3 seems to hurt the affine models in the valuation of long-maturity options.

Finally, the plots in the bottom row of Figure 7 show *RMSE* and bias for each model using eight volatility bins. To ensure meaningful comparisons, we define the volatility on a given day as the level of the CBOE's VIX volatility index. These plots illustrate the problems with the AGARCH(1, 1) models even more starkly. In particular, the *RMSE* plots indicate that these models perform similarly to the other models only when the VIX index is near its average over the sample period (i.e., 15.98%). Interestingly, the differences between the NGARCH(C) models on the one hand and the AGARCH(C) and NGARCH(1, 1) models on the other hand seem to be smaller than those in the moneyness and maturity dimensions depicted in the top and middle rows. Most notably, even with the nonaffine component models, a substantial bias clearly remains at high volatility levels.

5.4 Economic Assessment of Option Valuation Performance

We now turn to a more detailed analysis of the option valuation performance of the models over time. Toward this end, we regress the weekly option bias (defined as the weekly average market price less the weekly average option price) on some key economic variables: the VIX index, the weekly S&P 500 return, the weekly crude Brent Oil price, the 3-month T-bill rate, the credit spread (defined as the yield on corporate bonds rated Baa less the yield on Aaa bonds as rated by Moody's), and the term spread, defined as the difference between the yield on 10-year T-bond and the 3-month T-bill rate. We also include as regressors the weekly average moneyness, defined as index value over strike price (S/X), and the weekly average maturity in years. For these variables, averages are taken each week across the option contracts observed on the Wednesday of that week. The final regressor is the model-specific variance forecast for each model, defined as the average of the model's variance forecasts for the next month, as implied by the parameters given in Table 1.

Table 3 reports the results of the regressions of weekly option bias on the economic variables. The top row reports the average weekly bias (across the whole sample) for each model. t-statistics for each regressor are given, with the standard deviation for each regressor computed using White's robust variance matrix. Any t-statistic exceeding 2 in absolute value is in bold type. The bottom row gives the regression fit via the R-squared statistic. Most importantly, note that the R-squared values are quite high, suggesting that for these models, misspecification can be detected quite easily by analyzing model bias. Note that the explanatory power is particularly high in the affine GARCH(1, 1) models and lowest in the nonaffine component models.

Table 3. Regressing weekly bias on economic variables

	AGARCH-N		NGARCH-N		AGARCH-GED		NGARCH-GED	
	GARCH(1, 1)	Components	GARCH(1, 1)	Components	GARCH(1, 1)	Components	GARCH(1, 1)	Components
Average weekly bias	−0.9684	−0.3031	−0.1260	0.5500	−0.9745	−0.2186	0.0700	0.6467
Regressor				t-statistics using White's robust standard errors				
Constant	**−3.983**	**−3.247**	−1.497	−1.537	**−3.970**	**−3.117**	−1.581	−1.237
VIX	**10.559**	**10.345**	**9.520**	**10.978**	**10.326**	**10.947**	**9.511**	**11.142**
S&P 500 weekly return	−1.269	**−2.215**	−1.734	**−4.023**	−1.250	**−2.870**	−1.755	**−4.011**
Oil price	1.651	**3.648**	**6.077**	**5.745**	1.725	**3.494**	**6.281**	**5.873**
3-month T-bill rate	**2.993**	0.731	0.309	**−3.247**	**3.008**	0.322	0.054	**−3.408**
Credit spread	**7.548**	**7.233**	**4.724**	1.646	**7.564**	**6.794**	**4.553**	0.887
Term spread	**3.376**	0.790	0.076	**−2.748**	**3.292**	0.543	−0.261	**−2.772**
Average moneyness (S/X)	**2.049**	1.766	0.115	0.685	**2.053**	1.717	0.238	0.402
Average maturity (YTM)	−0.356	0.580	−1.844	**3.233**	−0.562	1.308	−0.914	**3.721**
Model variance forecast	**−5.950**	**−12.011**	**−15.830**	**−14.017**	**−5.787**	**−12.911**	**−16.046**	**−14.194**
Regression R-squared	0.8881	0.7582	0.7405	0.6124	0.8856	0.7432	0.7298	0.6112

NOTE: For each model we regress the weekly bias on a constant and various weekly economic variables, as well as the average weekly moneyness and maturity of the options in the sample. We also regress on the model-specific variance forecast. We report the t-statistic for each regressor using White's robust standard errors. Numbers in bold are larger than two in absolute value. The top row shows the average weekly bias and the bottom row reports the R-squared regression fit.

Downloaded by [University of Toronto Libraries] at 07:32 18 November 2014

The VIX is positive and significant for all models, and the variance forecast is negative and significant. The coefficient on the S&P 500 return is estimated to be negative for all models (the opposite sign of the VIX), but it is not always significant. The increase in the short-term rate, as well as the decline in the term and credit spreads, seem capable of explaining some of the upward bias in the affine model prices seen in the second half of the sample.

In summary, this specification analysis highlights some interesting differences between the models and provides insight into the models' strengths and weaknesses. These findings also suggest that building option pricing models with variance dynamics driven by key economic variables, such as credit spreads and oil prices, is a viable avenue for future research.

5.5 Alternative Estimation Strategies

So far, we have estimated the GARCH models on daily returns only and then used them for option valuation without letting the model parameters be driven in any way by the observed option prices. We now want to check the robustness of our results in two ways. First, because the return sample period (1962–2001) used here overlaps with the option sample period (1990–1995), we shorten the return sample period to end in 1989, just before the start of the option sample period. Second, we use options to estimate the weekly spot variance, h_t, minimizing the weekly option *RMSE* while keeping the model parameters fixed at the ML estimate values estimated on the 1962–1989 sample of daily index returns. These results are presented in Table 4 and Figure 8.

Panel A of Table 4 summarizes the valuation results using the ML estimation parameters from 1962–2001. The *RMSE* in the top row of Table 4 is simply repeated from the next to last row of Table 2. The second row of Table 4 reports the overall bias, which is close to 0 for all models. The third row reports the average spot volatility across the 313 option sample days. Because of the variance targeting used in ML estimation, these average volatilities are quite similar across models. Finally, the fourth row reports the standard deviation of the 313 spot variances. In keeping with the results in Figure 2, the volatility of variance is highest in the nonaffine models.

Panel B of Table 4 reports the same set of results using ML estimates of the GARCH parameters from daily returns from 1962 through 1989 rather than through 2001. Note that the option *RMSE* often is lower when parameters are estimated on returns observed through 1989 than when estimated on returns observed through 2001. Compared with the 2001 estimates, the 1989 estimates result in higher option *RMSE*s only in the two nonaffine component models. Whereas the evidence in favor of nonaffine component models weakens, the other overall conclusions from the 2001 estimates remain intact. The poorer option valuation performance of the nonaffine component models when using the shorter sample could be driven by the fact that the component models require a longer return sample to properly identify the components.

Panel C of Table 4 uses the GARCH parameters from ML estimation on returns up through 1989, but estimates the GARCH spot variance, h_t, each week by minimizing that week's option *RMSE* using a nonlinear least squares (NLS) technique. Comparing the pure MLE *RMSE*s in panel B with the hybrid *RMSE*s in panel C shows that the reduction in *RMSE* is dramatic in all models. The four nonaffine models now all have an *RMSE* of around \$1, compared with around 1.36 for the two affine component models and around \$2 for the GARCH(1, 1) models. The overall ranking of models from the pure ML estimation analysis remains largely intact.

Figure 8 elaborates further on this finding by plotting the weekly spot volatility from NLS (dots), along with the corresponding ML estimation–based spot volatilities (solid lines). The differences between the ML estimation–based and NLS-based results in Figure 8 are quite striking. In the affine GARCH(1, 1) models, the NLS optimizer forces the spot volatility to 0 in much of the second half of the sample to decrease the overpricing.

Table 4 also reports the *RMSE* between the annualized *RMSE*-optimal volatility and its ML-optimal counterpart. These numbers confirm the visual impression from Figure 8 and also corroborate some of our earlier findings. First, the nonaffine models have a much closer correspondence between option-implied and purely return-generated spot volatility. Second, the component structure reduces the volatility *RMSE* by well over 50% in the affine models and also quite substantially in the nonaffine models. Third, the GED shocks do not have much effect when judged by this metric either.

In the last four rows of Table 4, we split the 1990–1995 sample into two halves and report the option *RMSE* and bias for each half, using the NLS estimation results. Note that the AGARCH(1, 1) models are characterized by large negative bias in the second half of the sample, which leads to large *RMSE*s. Thus the overpricing persists even when the NLS optimization drives the spot variances to 0 in the second half of the sample.

Finally, it must be emphasized that the smaller NLS bias cannot be interpreted as suggesting the superiority of this type of exercise. The MLE setup clearly provides more challenges for any model, thereby automatically leading to a higher bias.

6. CONCLUSION AND DIRECTIONS FOR FUTURE WORK

We have assessed the ability of eight different GARCH models to fit daily return dynamics and their ability to match market prices of options. First, we considered component models versus GARCH(1, 1) models. Like Engle and Lee (1999), we found strong evidence in favor of component models from the standpoint of modeling daily return dynamics. When using option prices to assess the models, we also found strong evidence for the component structure in the affine GARCH models, but less so in the nonaffine models. Second, we considered nonaffine versus affine GARCH models. We compared the affine GARCH(1, 1) model with the nonaffine NGARCH(1, 1) model of Hsieh and Ritchken (2005), who found strong support for the nonaffine specification. Our results support their findings, and we also found that the nonaffine models outperform affine models when allowing for component structures and nonnormal shocks. Third, we considered conditionally normal versus conditionally nonnormal models. We found that assuming GED

Table 4. Alternative estimation strategies

	AGARCH-N		NGARCH-N		AGARCH-GED		NGARCH-GED	
	GARCH(1, 1)	Components	GARCH(1, 1)	Components	GARCH(1, 1)	Components	GARCH(1, 1)	Components
Panel A: Results from MLE on 1962–2001 sample								
Option *RMSE*, 1990–1995	2.6927	1.8138	1.5875	1.3820	2.6819	1.7404	1.4599	1.4270
Option bias, 1990–1995	−0.0423	−0.0149	−0.0077	0.0193	−0.0425	−0.0114	−0.0004	0.0229
Ann avr vol (%), 1990–1995	12.367	11.884	11.293	11.153	12.398	11.907	11.292	11.157
Ann vol of var (%), 1990–1995	0.7904	0.8763	1.0064	0.9758	0.7819	0.8587	1.0081	0.9753
Panel B: Results from MLE on 1962–1989 sample								
Option *RMSE*, 1990–1995	2.4750	1.6805	1.4347	1.4782	2.4163	1.6438	1.4021	1.5179
Option bias, 1990–1995	−0.0314	−0.0060	0.0043	0.0268	−0.0296	−0.0046	0.0095	0.0296
Ann avr vol (%), 1990–1995	12.442	11.871	11.218	11.086	12.428	11.904	11.235	11.107
Ann vol of var (%), 1990–1995	0.7485	0.8481	1.0122	0.9932	0.7283	0.8324	1.0087	0.9876
Panel C: Results from NLS estimation of GARCH spot variance								
Option *RMSE*, 1990–1995	2.0362	1.3555	1.0416	1.0076	1.9490	1.3731	1.0273	1.0143
Option bias, 1990–1995	−0.0174	0.0107	0.0058	0.0061	−0.0137	0.0118	0.0054	0.0055
Ann avr vol (%), 1990–1995	7.097	10.255	11.306	12.050	7.275	10.500	11.715	12.261
Ann vol of var (%), 1990–1995	2.5754	1.3651	1.1766	0.9814	2.4127	1.3083	1.2098	1.0068
RMSE of ann vol (%)	9.3485	3.7099	2.3055	1.6955	9.0147	3.4056	2.3297	1.7829
Option *RMSE*, 1990–1992	1.3531	1.1555	0.8042	0.9170	1.3226	1.2479	0.8390	0.9249
Option *RMSE*, 1993–1995	2.4156	1.4845	1.1852	1.0689	2.3008	1.4577	1.1453	1.0748
Option bias, 1990–1992	0.1499	0.1772	0.0684	0.0987	0.1611	0.2336	0.0544	0.0856
Option bias, 1993–1995	−0.9482	0.3863	0.2317	0.2225	−0.7770	0.3982	0.2232	0.2027

NOTE: Using the GARCH MLE paramaters from Table 1, panel A reports the overall option *RMSE* and bias, as well as the average model volatility on the option data days and the standard deviation of the model variance path on the option data days. Panel B reports the same statistics but using GARCH parameters estimated on the 1962–1989 sample instead. In panel C, we use NLS to estimate the *RMSE* optimal spot variance each week but rely on the GARCH MLE parameters from the 1962–2001 sample of returns. We also report the *RMSE* distance between the annualized MLE volatility path and the NLS optimal volatilities, as well as the option *RMSE* and bias split up into the first and second half of the sample.

Downloaded by [University of Toronto Libraries] at 07:32 18 November 2014

shocks for the daily asset returns greatly improves the fit of the all models to daily returns, but the improvement in option valuation is much less evident.

The empirical results suggest some viable directions for future research. First, it remains to be seen whether the differences in performance between models are confirmed when using model parameters estimated from option prices, or when using an integrated analysis that uses option prices as well as underlying returns (see Bates 2000; Chernov and Ghysels 2000; Eraker 2004). The analysis in Table 4 suggests that the relative performance of the models is comparable when the spot volatility is estimated from options rather than filtered from returns.

Second, it would be interesting to expand the analysis of nonnormal shocks to a wider class of distributions. Toward this end, Christoffersen, Heston, and Jacobs (2006) developed an inverse-Gaussian GARCH model, Duan, Ritchken, and Sun (2006) suggested augmenting GARCH models with jumps, and Lehnert (2003) applied an EGARCH model with skewed GED shocks.

Third, we have restricted attention to European-style options on the S&P 500 index. It would be interesting to apply the GARCH modeling framework to some of the many American-style contracts traded in the derivatives markets. Ritchken and Trevor (1999) and Stentoft (2005) have provided fast numerical techniques for GARCH option valuation with early exercise.

Finally, it would be interesting to compare the range of discrete-time GARCH models considered here with continuous-time stochastic volatility models. Bates (1996), Bakshi, Cao, and Chen (1997), and Eraker (2004) have studied stochastic volatility models with jumps; Taylor and Xu (1994) have studied multifactor stochastic volatility models; and Bates (2000) has analyzed models with Poisson jumps and multiple

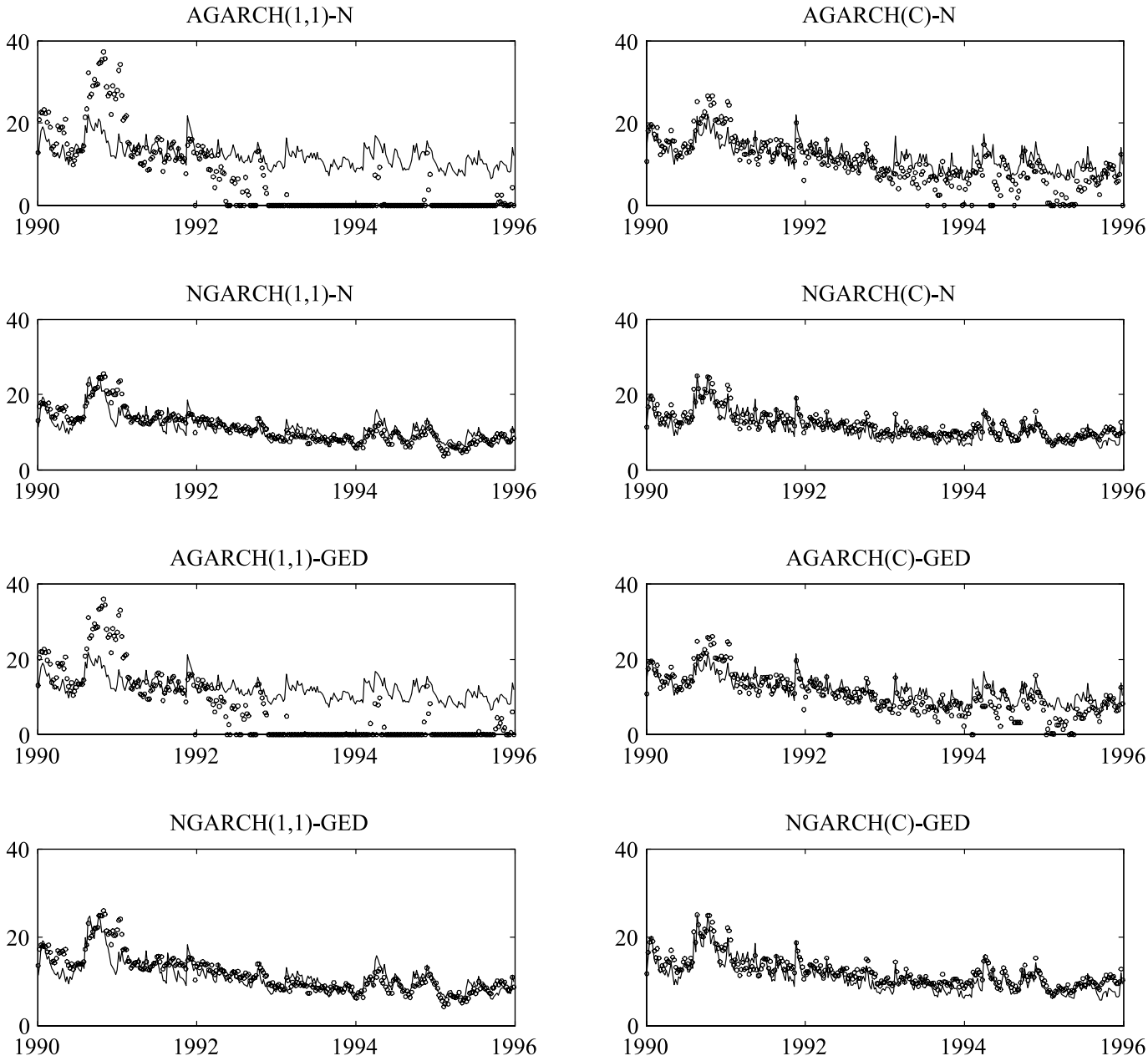

Figure 8. *RMSE*-optimal spot volatility estimated weekly by NLS. The dots show the weekly *RMSE*-optimal GARCH annualized spot volatilities, $100 * \sqrt{252 * h_t}$, estimated by NLS. The annualized ML estimation–optimal volatility path is show in solid lines.

Downloaded by [University of Toronto Libraries] at 07:32 18 November 2014

volatility factors. Comparing GARCH and SV models for the purpose of option valuation may provide more insight into the strengths and weaknesses of the various models.

ACKNOWLEDGMENTS

Christoffersen and Jacobs are also affiliated with CIRANO and CIREQ, and would like to thank FQRSC, IFM2, and SSHRC for financial support. Dorion was supported by fellowships from FQRNT and IFM2, and Wang was supported by fellowships from McGill University and FQRSC. We would also like to thank Tim Bollerslev for suggesting this line of research.

[Received November 2006. Revised December 2008.]

REFERENCES

Adrian, T., and Rosenberg, J. (2008), "Stock Returns and Volatility: Pricing the Long-Run and Short-Run Components of Market Risk," *Journal of Finance*, 63, 2997–3030. [483]

Bakshi, C., Cao, C., and Chen, Z. (1997), "Empirical Performance of Alternative Option Pricing Models," *Journal of Finance*, 52, 2003–2049. [494,500]

Bates, D. (1996), "Jumps and Stochastic Volatility: Exchange Rate Processes Implicit in Deutsche Mark Options," *Review of Financial Studies*, 9, 69–107. [500]

——— (2000), "Post-87 Crash Fears in S&P500 Futures Options," *Journal of Econometrics*, 94, 181–238. [500]

Black, F. (1976), "Studies of Stock Price Volatility Changes," in *Proceedings of the 1976 Meetings of the Business and Economic Statistics Section*, Alexandria, VA: American Statistical Association, pp. 177–181. [484]

Bollerslev, T. (1986), "Generalized Autoregressive Conditional Heteroskedasticity," *Journal of Econometrics*, 31, 307–327. [483]

Bollerslev, T., and Mikkelsen, H. O. (1999), "Long-Term Equity Anticipation Securities and Stock Market Volatility Dynamics," *Journal of Econometrics*, 92, 75–99. [483,485]

Bollerslev, T., and Wooldridge, J. (1992), "Quasi-Maximum Likelihood Estimation and Inference in Dynamic Models With Time Varying Covariances," *Econometric Reviews*, 11, 143–172. [487]

Chernov, M., and Ghysels, E. (2000), "A Study Towards a Unified Approach to the Joint Estimation of Objective and Risk Neutral Measures for the Purpose of Option Valuation," *Journal of Financial Economics*, 56, 407–458. [500]

Christoffersen, P., and Jacobs, K. (2004), "Which Volatility Model for Option Valuation?" *Management Science*, 50, 1204–1221. [483]

Christoffersen, P., Heston, S., and Jacobs, K. (2006), "Option Valuation With Conditional Skewness," *Journal of Econometrics*, 131, 253–284. [500]

Christoffersen, P., Jacobs, K., Ornthanalai, C., and Wang, Y. (2008), "Option Valuation With Long-Run and Short-Run Volatility Components," *Journal of Financial Economics*, 90, 272–297. [483,485,495]

Duan, J.-C. (1995), "The GARCH Option Pricing Model," *Mathematical Finance*, 5, 13–32. [483,485,489,492]

——— (1999), "Conditionally Fat-Tailed Distributions and the Volatility Smile in Options," manuscript, Hong Kong University of Science and Technology. [483,484,486,489]

Duan, J.-C., and Simonato, J.-G. (1998), "Empirical Martingale Simulation for Asset Prices," *Management Science*, 44, 1218–1233. [493]

Duan, J.-C., Ritchken, P., and Sun, Z. (2006), "Approximating GARCH-Jump Models, Jump-Diffusion Processes, and Option Pricing," *Mathematical Finance*, 16, 21–52. [500]

Engle, R. (1982), "Autoregressive Conditional Heteroskedasticity With Estimates of the Variance of UK Inflation," *Econometrica*, 50, 987–1008. [483]

Engle, R., and Lee, G. (1999), "A Permanent and Transitory Component Model of Stock Return Volatility," in *Cointegration, Causality, and Forecasting: A Festschrift in Honor of Clive W.J. Granger*, eds. R. Engle and H. White, New York: Oxford University Press, pp. 475–497. [483,485,499]

Engle, R., and Ng, V. (1993), "Measuring and Testing the Impact of News on Volatility," *Journal of Finance*, 48, 1749–1778. [483,485]

Eraker, B. (2004), "Do Stock Prices and Volatility Jump? Reconciling Evidence From Spot and Option Prices," *Journal of Finance*, 59, 1367–1403. [500]

Hamilton, J. (1994), *Time Series Analysis*, Princeton, NJ: Princeton University Press. [486]

Heston, S., and Nandi, S. (2000), "A Closed-Form GARCH Option Pricing Model," *Review of Financial Studies*, 13, 585–626. [483-485,490,493]

Hsieh, K., and Ritchken, P. (2005), "An Empirical Comparison of GARCH Option Pricing Models," *Review of Derivatives Research*, 8, 129–150. [483,496,499]

Jones, C. (2003), "The Dynamics of Stochastic Volatility: Evidence From Underlying and Options Markets," *Journal of Econometrics*, 116, 181–224. [484]

Lehnert, T. (2003), "Explaining Smiles: GARCH Option Pricing With Conditional Leptokurtosis and Skewness," *Journal of Derivatives*, 10, 27–39. [483,500]

Maheu, J. (2005), "Can GARCH Models Capture the Long-Range Dependence in Financial Market Volatility?" *Studies in Nonlinear Dynamics and Econometrics*, 9, Article 1. [483]

Nelson, D. B. (1991), "Conditional Heteroskedasticity in Asset Returns: A New Approach," *Econometrica*, 59, 347–370. [486]

Ritchken, P., and Trevor, R. (1999), "Pricing Options Under Generalized GARCH and Stochastic Volatility Processes," *Journal of Finance*, 54, 377–402. [500]

Stentoft, L. (2005), "Pricing American Options When the Underlying Asset Follows GARCH Processes," *Journal of Empirical Finance*, 12, 576–611. [500]

Taylor, S., and Xu, X. (1994), "The Term Structure of Volatility Implied by Foreign Exchange Options," *Journal of Financial and Quantitative Analysis*, 29, 57–74. [500]

Theodossiou, P. (2001), "Distribution of Financial Asset Prices, the Skewed Generalized Error Distribution, and the Pricing of Options," working paper, Rutgers University, School of Business. [483]

Downloaded by [University of Toronto Libraries] at 07:32 18 November 2014